EurJOC
European Journal of Organic Chemistry

Full Papers
doi.org/10.1002/ejoc.202100848

Chemistry Europe
European Chemical Societies Publishing

Special Collection

Bidirectional Synthesis, Photophysical and Electrochemical Characterization of Polycyclic Quinones Using Benzocyclobutenes and Benzodicyclobutenes as Precursors

Amr Mohamed Abdelmoniem,[a, b] Ismail Abdelshafy Abdelhamid,[b] and Holger Butenschön*[a]

In Memory of Professor Klaus Hafner

Quinones have widespread applications in view of their interesting chemical and photophysical features. On the other hand, benzocyclobutenes (BCBs) are generally masked reactive dienes suitable for the [4+2] cycloaddition reactions. Here, benzocyclobutenes and benzodicyclobutenes (BDCBs) were prepared and further reacted with benzoquinone and naphthoquinone in order to obtain some new polycyclic quinones with highly extended π systems, namely, 6-bromo-5,8-dimethoxyanthracene-1,4-dione, 2,9-dibromo-1,4,8,11-tetramethoxypentacene-6,13-dione, 9-bromo-7,10-dimethoxytetracene-5,12-dione, 3,10-dimethoxycyclobuta[*b*]anthracene-1,5,8(2*H*)-trione, 6,10,17,21-tetramethoxynonacene-1,4,8,12,15,19-hexaone, and 3,12-dimethoxycyclobuta[*b*]tetracene-1,5,10(2*H*)-trione. In addition to their spectroscopic characterization the new compounds are investigated by UV and fluorescence spectroscopy, cyclic voltammetry, and DFT calculations.

Introduction

The Diels-Alder cycloaddition is one of the most important strategies for the regio- and stereoselective synthesis of organic homo- and hetero-polycycles.[1–7] Over the years, the reaction has proven to be a powerful tool for the selective synthesis of complex natural products and biologically active molecules.[8–12] Quinones were found to be typical electron poor dienophiles in cycloaddition reactions.[13–17] In addition, quinone structures are widely abundant in redox-active natural compounds associated with a number of biological processes like photosynthesis in plants and bacteria,[18–20] coenzyme Q functions,[21–24] vitamins K[25–29] and E[30–32] activities. They show marked anti-oxidant,[33–34] anti-inflammatory,[35–37] antibiotic,[38–41] and antitumoral[42–45] activities as well. Some FDA-approved quinone drugs are depicted in Figure 1.

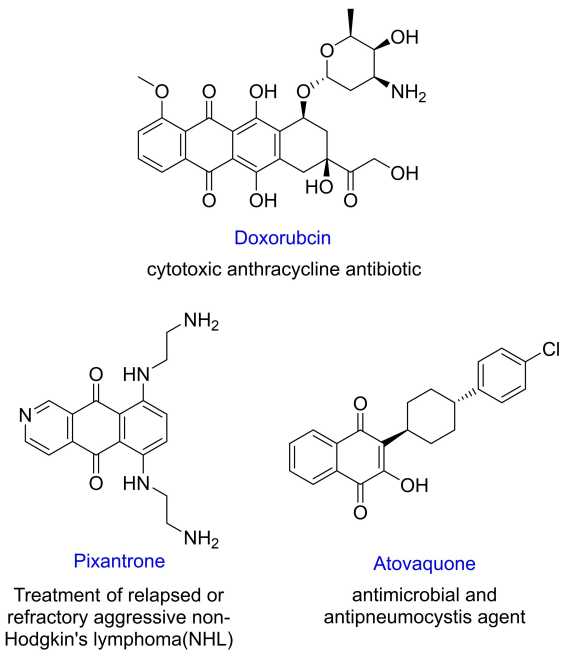

Figure 1. Some FDA-approved quinone drugs.

Generally, several approaches have been elaborated for the synthesis of extended quinones. Among them, the bidirectional synthesis of extended quinones seems to be particularly attractive. Figure 2 summarizes some selected important bidirectional syntheses of quinones, including, A: the condensation reaction of aromatic *o*-dicarboxaldehydes with 1,4-cyclohexanedione,[46–49] B: the 1,4-cycloadditions of bis-dienes with a quinone,[50–52] and C: the cycloaddition of aromatic quinones with in situ formed dienes from tetra- or hexa

[a] *Dr. A. Mohamed Abdelmoniem, Prof. Dr. H. Butenschön*
Institut für Organische Chemie
Leibniz Universität Hannover
Schneiderberg 1B, 30167 Hannover, Germany
E-mail: holger.butenschoen@mbox.oci.uni-hannover.de
https://www.oci.uni-hannover.de/de/arbeitsgruppen/ag-butenschoen/
[b] *Dr. A. Mohamed Abdelmoniem, Prof. Dr. I. Abdelshafy Abdelhamid*
Department of Chemistry
Faculty of Science, Cairo University
12613 Giza, A. R. Egypt

Supporting information for this article is available on the WWW under https://doi.org/10.1002/ejoc.202100848

Part of the "Special Collection in Memory of Klaus Hafner".

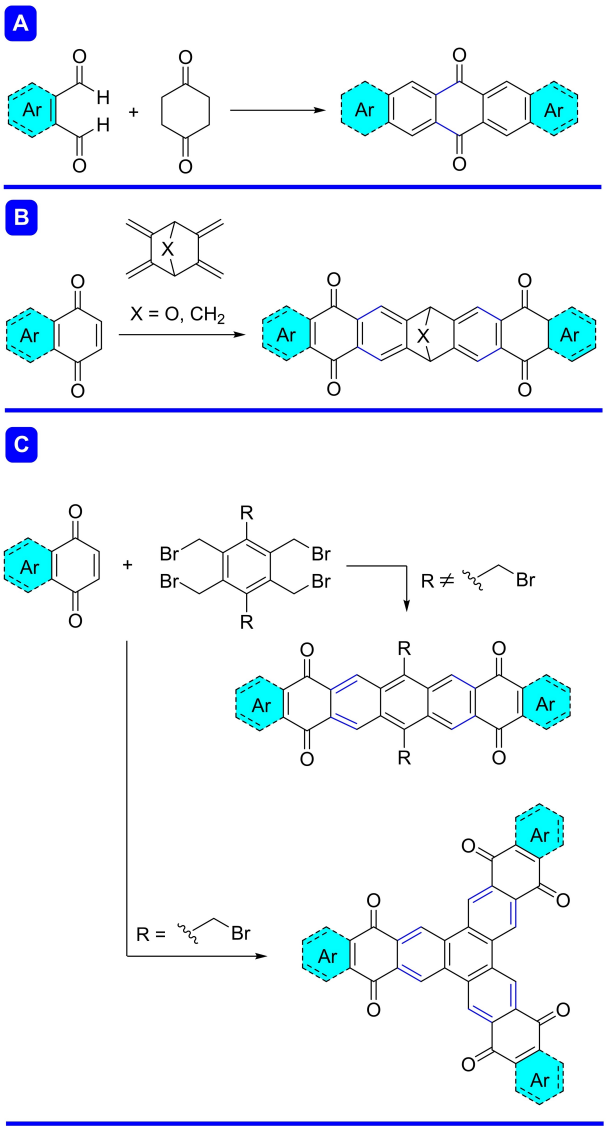

Figure 2. Some bidirectional synthetic approaches to extended quinones.

(bromomethyl)benzene to form linear or star-shaped quinones.[53–55]

On the other hand, BCBs can be considered as masked thermally stabilized *o*-xylylenes via in situ electrocyclic ring opening (Figure 3).[56–58]

In a previous work,[59] the reactivity of BCBs towards *N*-methylmaleimide forming some interesting benzo[1,2-*f*:4,5-*f'*] diisoindoles was studied (Scheme 1). The reaction of BCB **1** with *N*-methylmaleimide (**2**) afforded the desired benzo[*f*]isoindole-1,3(2*H*)-dione **5** in low yield (15%) besides more than 60% yield of unaromatized products **3** and **4**. In case of the reaction of benzodicyclobutene (BDCB) **6** with *N*-methylmaleimide (**2**), the targeted benzo[1,2-*f*:4,5-*f'*]diisoindole derivative **11** could only be isolated in 10% yield along with the formation of other monoaddition and unaromatized dicycloaddition products **7**–**10** in a total yield of 68%. The main reason for the low yields of the desired products clearly is the lack of an internal oxidant

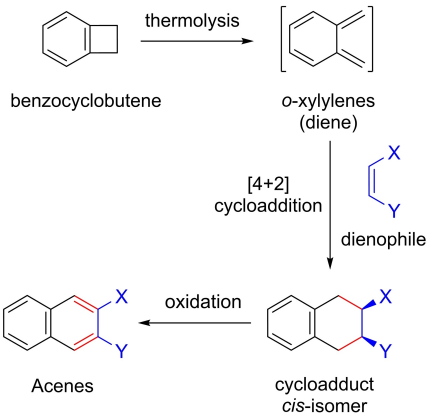

Figure 3. Benzocyclobutene as precursor of *o*-xylylene in the Diels-Alder reaction with a *cis*-dienophile followed by oxidation to the acene.

impeding the possible formation of aromatized products. However, the use of an internal oxidant appears not to be practical as it may react with the sensitive BCB ring. In this context, here we report on the reactivity of BCBs and BDCBs towards benzoquinone and naphthoquinone, which serve as both, dienophile and internal oxidant.

Results and Discussion

Synthesis and characterization

The synthetic procedures of starting materials BCB **18**, BDCBs **19** and **20** are depicted in Scheme 2. 1,4-Dibromo-2,5-dimethoxybenzene (**12**) was reacted with an excess of ketene dimethylacetal (**13**) (5 equiv.) in the presence of sodium amide (4 equiv.) in THF at reflux for 24 h according to our previously reported procedure.[60] After a careful chromatographic separation, three main products **1**, **14**, and **6** were obtained in 5%, 55% and 25% yield, respectively, besides other byproducts (16%). To circumvent the poor yield of **1**, this compound was prepared under modified reaction conditions by reaction of **12** with ketene dimethylacetal (**3**) (1.25 equiv.) in presence of sodium amide (1 equiv.). In this case, compound **1** was obtained in 55% yield. BCB **18** was prepared from BCB **1** via hydrolysis to BCB **15**[60] followed by reduction with sodium borohydride. Similarly, BDCDs **19** and **20** were synthesized starting from BDCBs **14** and **6** via hydrolysis to **16**[60] and **17**[60] respectively, followed by reduction. The chemical constitutions of BCB **1**, BDCBs **19**, and **20** were confirmed spectroscopically. Surprisingly, ^{1}H NMR spectroscopy revealed that BDCB **19** appeared as an inseparable mixture of diastereomers while BDCB **20** furnished two distinct diastereomers of different solubilities: **20a** (partially insoluble in chloroform) and **20b** (soluble in chloroform).

This method has the advantage of obtaining BCBs and BDCBs in good yields. However, the difficult availability of ketene precursor **3** and the tedious chromatographic purification are problematic. Adopting a similar procedure to that

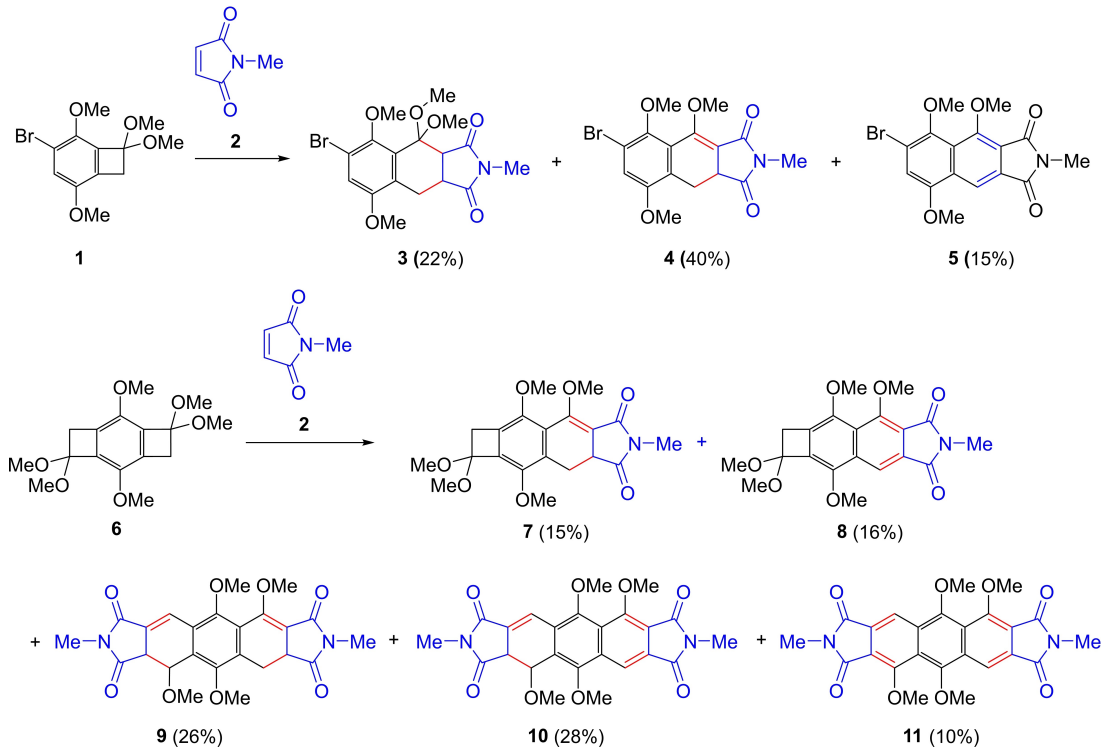

Scheme 1. The reaction of BCB **1** and BDCB **6** with *N*-methylmaleimide (**2**).[59]

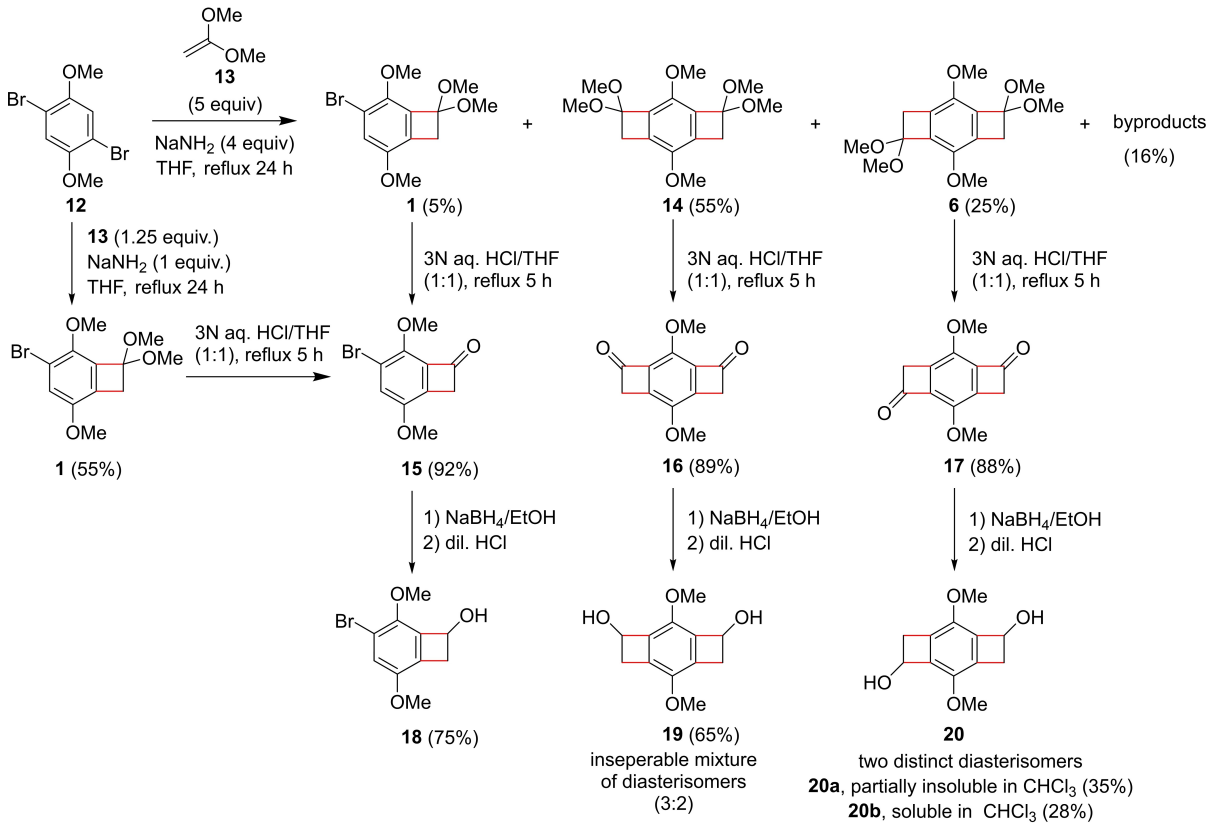

Scheme 2. Syntheses of starting materials BCB **18**, BDCBs **19** and **20**.

reported by Dong et al.[61] we managed to obtain BCB **18** directly in a single operation by the action of butyllithium and lithium 2,2,6,6-tetramethylpiperidide (LiTMP) on a solution of **12** in THF (Scheme 3).[62] In this reaction, the cycloreversion of lithiated THF **21** dissociates ethene (**22**) giving the intermediate enolate **23**. The subsequent [2 + 2] cycloaddition reaction of **23** (3 equiv.) with dibromo compound **12** (1.0 equiv.) induced by LiTMP (1.5 equiv.) furnishes **24**, which is then hydrolyzed to form BCB **18** in 61 % yield.

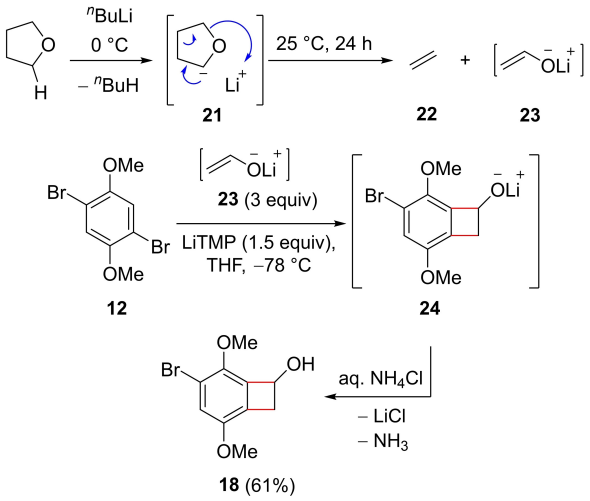

Scheme 3. An alternative method for the synthesis of BCB **18**.

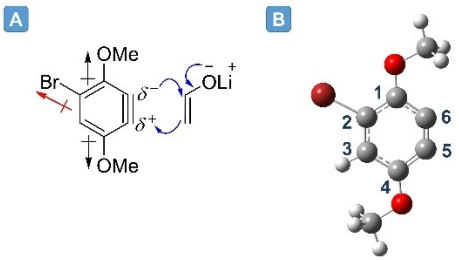

Figure 4. Regioselectivity of aryne [2 + 2] cycloaddition. A) The -I effect of Br on the triple bond. B) The optimized calculated structure of the benzyne intermediate at B3LYP/6-31 + + (*d,p*) level of theory.

Table 1.

Atom	NPA charge	Natural electron configuration	Idealized Hybridization
C6	−0.051	$1\,s^2 2\,s^{0.97}2p^{3.07}4\,s^{0.01}4p^{0.01}$	sp^2
C5	0.052	$1\,s^2 2\,s^{0.95}2p^{2.98}4p^{0.01}$	sp^2
C4	0.244	$1\,s^2 2\,s^{0.84}2p^{2.89}3d^{0.01}4p^{0.02}$	sp^2
C3	−0.331	$1\,s^2 2\,s^{0.97}2p^{3.33}4p^{0.01}$	sp^2
C2	−0.160	$1\,s^2 2\,s^{0.97}2p^{3.17}3p^{0.02}$	sp^2
C1	0.226	$1\,s^2 2\,s^{0.84}2p^{2.90}3\,s^{0.01}3d^{0.01}4p^{0.01}$	sp^2
Bond lengths [Å]		Bond angles [°]	
C5-C6	1.25	C1-C6-C5	125.6
C2-C3	1.39	C4-C5-C6	129.5
C4-C5	1.39	C3-C4-C5	109.4
C5-C6	1.41	C2-C3-C4	121.9
C1-C6	1.41	C1-C2-C3	123.9
C1-C2	1.41	C2-C1-C6	110.1

The origin of regioselectivity can roughly be rationalized as the dipole moments of both C–OMe cancel each other while that of C–Br (-I inductive effect) is not cancelled. Thus, a partial positive charge is generally generated at the carbon in the *para* position, while a partial negative charge originates at the *meta* carbon atom (Figure 4A). This is further evidenced by DFT calculations, which show that the more nucleophilic terminus of the C3-C4 bond is the carbon atom C3 at the *meta* position to Br atom. The optimized structure of the benzyne intermediate (Figure 4B) appears as a resonance contributor, in which the electron density at C3-C4 is delocalized across the ring affecting the electron densities at C2-C3 and C4-C5 as anticipated from their bond lengths (Table 1). The natural electronic configuration of valence orbitals of carbon atoms of the ring explains the idealized sp^2 hybridization of all carbon atoms. The nucleophilic addition preferably occurs at the more distorted carbon atom C4 (angle C3-C4-C5 = 129.5°) according to the aryne distortion model.[63]

The cycloaddition reaction of BCB **18** with BQ (**25**) was then investigated. Two products were successfully isolated in pure form after chromatographic separation: 6-Bromo-5,8-dimethoxyanthracene-1,4-dione (**26**), which results from the single cycloaddition of BCB **18** to one double bond of BQ (**25**), and either 2,9- or 2,10-dibromo-1,4,8,11-tetramethoxypentacene-6,13-dione, formed via the *syn* or the *anti* twofold cycloaddition of two equivalents of BCB **18** to either one of the double bonds of BQ (**25**), respectively (Scheme 4).

This reaction was examined in several solvents under different reaction conditions of conventional and microwave (μW) heating (Table 2). The best conditions found were the conventional heating in toluene at 120 °C in a sealed tube for 24–48 h and the microwave heating in toluene in a sealed tube

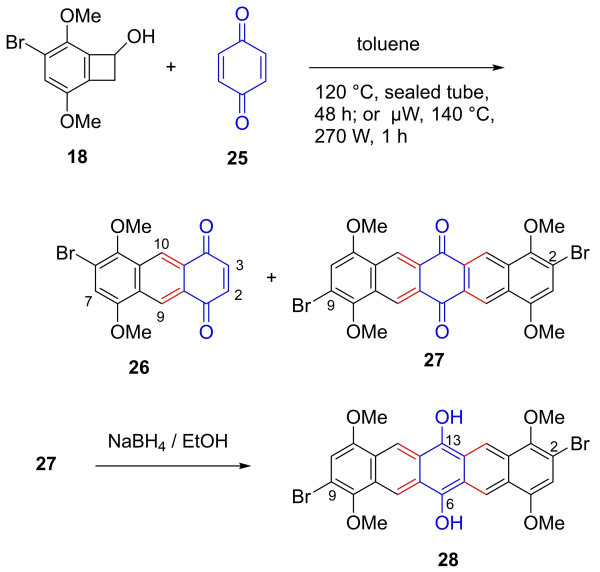

Scheme 4. The reaction of BCB **18** with 1,4-benzoquinone (**25**). Reaction conditions: BCB **18** (1 mmol), BQ (**25**) (4.6 mmol), toluene, 120 °C, sealed tube, 48 h, (**26**: 38 %, **27**: 22 %) or: μW, 140 °C, 270 W, 1 h, (**26**: 52 %, **27**: 26 %). Reduction of **27**: **27** (0.017 mmol), $NaBH_4$ (0.105 mmol), EtOH, 25 °C, 3 h, (**28**: 38 %).

Table 2. Optimization of the reaction of BCB **18** with 1,4-benzoquinone (**25**).[a]

Entry	Solvent	Conditions	T [°C] [b]	t [h]	Yield [c] **26** [%]	Yield [c] **27** [%]
1	THF	reflux	60	8	–	–
2	Benzene	reflux	80	8	–	–
3	Toluene	sealed tube, conventional heating	120	24	49	–
4	Toluene	sealed tube, conventional heating	120	48	38	22
5	1,2-dichlorobenzene	sealed tube, conventional heating	140	24	45	6
6	1,2-dichlorobenzene	sealed tube, conventional heating	140	48	35	17
7	Nitrobenzene	sealed tube, conventional heating	180	24	27	3
8	Nitrobenzene	sealed tube, conventional heating	180	48	35	18
9	Toluene	sealed tube, μW, 270 W	140	0.25	15	–
10	Toluene	sealed tube, μW, 270 W	140	0.5	24	7
11	Toluene	sealed tube, μW, 270 W	140	0.75	43	16
12	Toluene	sealed tube, μW, 270 W	140	1	52 (54)[d]	26 (24)[d]
13	Toluene	sealed tube, μW, 270 W	140	1.5	47	22
14	1,2-dichlorobenzene	sealed tube, μW, 270 W	160	1	48 (49)[d]	24 (23)[d]
15	Nitrobenzene	sealed tube, μW, 270 W	190	1	38 (40)[d]	23 (21)[d]

[a] The molar ratio of reactants: BCB **14** (1 mmol), 1,4-BQ (**25**, 4.6 mmol). [b] Heating bath temperature. [c] Isolated yield. [d] added LiCl (40 mol%).

at 140 °C for 1 h. Increasing the temperature further in other solvents like nitrobenzene or 1,2-dichlorobenzene did not lead to a noticeable increase in yield. Instead, an unidentified charry substance was obtained probably due to thermal decomposition of products. Also, changing the microwave irradiation time from 0.25 h to 1.5 h (Entries 9–13) was tried, and the best time was 1 h. Addition of LiCl (40 mol%) led only to a slight increase in the yield of the mono-cycloaddition product **26** under microwave (μW) irradiation.

Changing the molar ratio of BCB **18** to 1,4-benzoquinone (**25**) in a gradient from 2.5:1 to 0.75:1 was tried. A gradual increase in the yield of the monocycloaddition product **26** was observed until its maximum at the ratio 1:1 (Table 3).

26 was characterized spectroscopically. The mass spectrum of **26** displayed peaks (1:1) at $m/z = 346$ $[M]^+$ and 348 $[M+2]^+$ indicating the presence of one Br atom, in addition to a base peak at $m/z = 331$, 333 corresponding to the fragmentation of a methyl group. The IR spectrum revealed a characteristic band at $\tilde{\nu} = 1671\ cm^{-1}$ for the C=O stretching vibration. The ^1H as well as the ^{13}C NMR spectrum are in full accord with the constitution of **26**. On the other hand, the presence of two bromine atoms in **27** is verified from the isotopic molecular ion cluster at $m/z =$ 584, 586 and 588 (1:2:1). The IR spectrum showed a characteristic C=O stretching band at $\tilde{\nu} = 1673\ cm^{-1}$. However, the only available spectroscopic tool to identify whether the bromo substituents are located at the 2,9 or at the 2,10 positions in compound **27** was ^{13}C NMR spectroscopy, where one signal for the carbonyl carbon atoms would appear if the bromo substituents were located at the 2,9 positions, while two signal would be expected they were located at the 2,10 positions. Unfortunately, a well-resolved ^{13}C NMR spectrum could not be obtained due to the low solubility of compound **27** in almost all available deuterated solvents ($CDCl_3$, acetone-d_6, DMSO-d_6) even at elevated temperature (40 °C). Attempts to obtain a single crystal for compound **27** were also in vain. Therefore, the reduction of compound **27** was tried with sodium borohydride in order to get a reduction product **28** of a better solubility. The ^1H NMR spectrum did not show the peak of the hydroxy protons and showed only one signal integrated for 12 protons for the methoxy groups. However, the reduction of the carbonyl groups in **27** was confirmed by the IR and ^{13}C NMR spectra, which indicated the absence of carbonyl groups. In addition, the ^{13}C NMR spectrum displayed two different signals for methoxy groups and one signal for *C*-OH at $\delta = 153.6$ ppm, and thus it is in accord with a 2,9-dibromo substitution in **28** as well as in **27**.

Table 3. Effect of the molar ratio of reactants (BCB **18** : BQ **25**) on the yield of the monocycloaddition product **26**.

Entry	BCB : BQ	Yield [%] Conventional heating (120 °C, 48 h)	Microwave (140 °C, 1 h)
	2.5:1	49	52
2	2:1	51	54
3	1.5:1	56	57
4	1:1	64	66
5	0.75:1	57	58

Generally, the reaction is greatly facilitated if conducted in a sealed tube at a temperature higher than toluene reflux temperature at normal pressure. A plausible mechanism hence involves the ring-opening of the cyclobutene ring in BCB **18** to the *o*-xylylene **29**, which undergoes [4+2] cycloaddition reaction with BQ (**25**) to form the adduct **30**, which eliminates water and is further oxidized to form the mono-cycloaddition product **26**. Anthra-1,4-quinone **26** can similarly undergo a subsequent [4+2] cycloaddition reaction with another *o*-xylylene intermediate **29** giving the pentacene-6,13-dione **27** (Scheme 5). The oxidant seems to be either oxygen from the air or benzoquinone itself. Use of freshly distilled toluene under argon and purging the reaction mixture with argon before conventional or microwave heating did not affect the fully aromatized nature of products **26** and **27**. This, in addition to the presence hydroquinone impurities during chromatographic separation, suggests that the oxidizing agent is benzoquinone.

It is noteworthy that anthracene-1,4-dione is a common fragment in various quinoid natural products such as rufooliva-

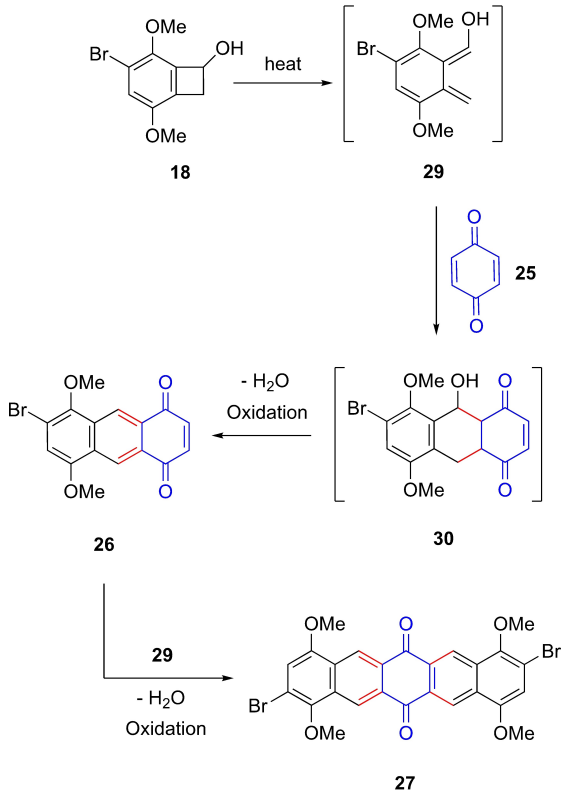

Scheme 5. A plausible mechanism for the formation of 1,4-anthraquinone **26** and pentacene-6,13-dione **27**.

cin B, presengulone, and sengulone.[64–65] Such compounds are shown to prevent macromolecule synthesis such as the biosynthesis of RNA or polypeptides in living cells and evoke interesting bioactivity as antiplasmodial, antibiotics, and antitumor agents.[66–68] On the other hand, pentacenes in virtue of their remarkable electronic properties are benchmark in the field of organic electronic devices.[69–70]

Analogously, tetracene-5,12-dione **32** was obtained as the sole product by ring opening / cycloaddition of BCB **18** with 1,4-naphthoquinone NQ (**31**) at elevated temperature (Scheme 6). The constitution of **32** was confirmed spectroscopically. The mass spectrum shows molecular ion peaks (1 : 1) at *m/z* = 396 $[M]^+$ and 398 $[M+2]^+$ due to the presence of one Br atom. The IR spectrum revealed a characteristic C=O stretching band at $\tilde{\nu}$ = 1672 cm^{-1}. The ^1H and ^{13}C NMR spectra are in full accord with the proposed constitution.

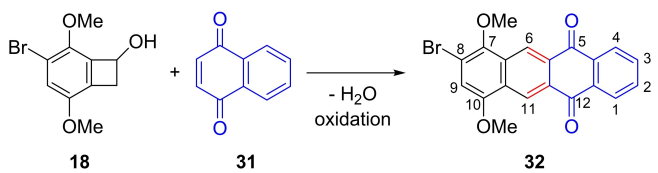

Scheme 6. Synthesis of tetracene-5,12-dione **32**. Reaction conditions: **18** (1.0 mmol), NQ (**31**) (4.6 mmol), toluene, 120 °C, sealed tube, 48 h (47 %) or: μW, 140 °C, 270 W, 1 h (58 %).

It should be noted that tetracene derivatives possess interesting optoelectronic properties, e.g. as organic light-emitting field-effect transistors (OLETs).[71–73] Tetracene-5,12-dione is the oxidized form of the core structure of anthracycline antibiotics[74–75] such as doxorubicin and daunorubicin, which were clinically proven to be effective antitumor reagents against acute leukemia, breast carcinomas, Hodgkin's disease, sarcomas and lymphomas.[76–77]

Encouraged by these results, we tried conducting this reaction scheme using BDCBs **19** and **20** aiming at higher acenes. Thus, the cycloaddition reaction of either BDCB **19** or **20** with benzoquinone (**25**) was carried out under conventional heating as well as under microwave irradiation conditions and was anticipated to finally yield pentacene-1,4,9,12-tetraone (**33**). A careful chromatographic separation of the crude product afforded different fractions. Besides the residual fractions of BQ, and BDCBs and their oxidized products (ca. 10 % yield),[50] two interesting fractions could be separated and characterized. However, none of the isolated fractions corresponds to the target product **33**.

The main fraction after isolation and purification was characterized spectroscopically as cyclobuta[*b*]anthracene-1,5,8(2*H*)-trione derivative **36**. The IR spectrum clearly showed the absence of hydroxy groups and presence of two close C=O stretching bands at $\tilde{\nu}$ = 1658, 1665 cm^{-1}. The ^1H NMR spectrum of this compound showed a characteristic singlet at δ = 5.00 (2H) ppm assigned to the cyclobutene CH_2 protons. It displayed also two singlets at δ = 3.97 (3H) ppm and δ = 4.07 (3H) ppm due to the two methoxy groups, two singlets at δ = 7.12 ppm (2H) for H6 and H7, and at δ = 8.85 ppm (2H) for H4 and H9. The formation of the cyclobuta[*b*]anthracene-1,5,8(2*H*)-trione **36** can be rationalized by a [4+2] cycloaddition of in situ generated *o*-xylylene **34** to BQ (**25**) followed by loss of water and oxidation to **35** and further by the oxidation of the secondary alcohol group to yield the ketone **36** in up to 41 % yield (Scheme 7).

Another fraction could be isolated and identified. The ^1H NMR spectrum featured a singlet at δ = 4.02 ppm (12H) for methoxy protons besides a set of singlets at δ = 6.92 (4H), 7.08 (4H), and 9.02 (4H) ppm for aryl protons. The IR spectrum showed two characteristic C=O stretching bands at $\tilde{\nu}$ = 1614, 1665 cm^{-1}. A proposed structure is nonacene-1,4,8,12,15,19-hexaone (**40**) (Scheme 8). The highly symmetric constitution of **40** could further be verified by its ^{13}C NMR spectrum, which showed a set of 11 signals: One characteristic signal for the methoxy carbon atoms at δ = 55.9 ppm; two signals at δ = 173.6 [C8(19)], 184.8 [C1(4, 12, 15)] ppm assigned to carbonyl carbon atoms; three signals for aromatic C–H carbon atoms at δ = 107.5 [C7(9, 18, 20)], 123.5 [C5(11, 16, 22)], 140.0 [C2(3, 13, 14)] ppm; signals for quaternary aromatic carbon atoms at δ = 127.6 [C6a(9a, 17a, 20a)], 128.1 [C5a(10a, 16a, 21a)], 130.7 [C4a(11a, 15a, 22a)], 135.2 [C7a(8a, 18a, 19a)], and 150.9 [C6(10,17,20)] ppm. On the other hand, the EI mass spectrum of **40** did not show a molecular ion peak. However, it revealed a peak at *m/z* = 663 $[M+H-C_2H_2]^+$ corresponding to the fragmentation of an ethyne molecule from $[M+H]^+$.

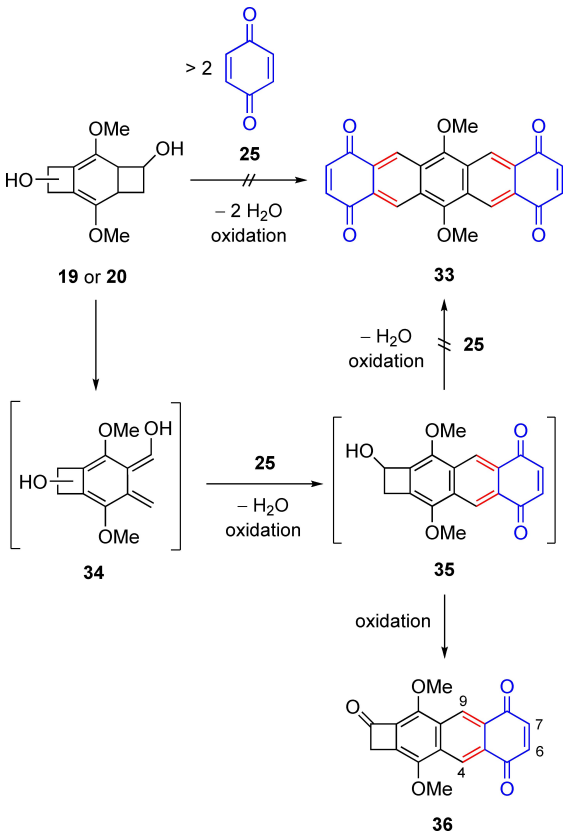

Scheme 7. Synthesis of cyclobuta[*b*]anthracene-1,5,8(2H)-trione **36**. Reaction conditions: **19** or **20** (1.0 mmol), BQ (**25**) (2.5 mmol), toluene, 120 °C, sealed tube, 48 h (34%) or: μW, 140 °C, 270 W, 1 h (41%).

goes loss of water and oxidation to diol **38**. Ring-opening of **38** affords bis-diene **39**, which undergoes further [4+2] cycloadditions to two equivalents of BQ (**25**) to form nonacene-1,4,8,12,15,19-hexaone (**40**). It has to be noted that we could observe the formation of **40** in a very low yield (5–7%) only in the case of microwave heating. This reflects the unlikeness of the five-component successive cycloaddition reaction of two equivalents of BDCB **17** or **19** with three equivalents of BQ (**25**) in a tandem way. The reaction comprises the formation of four new benzene rings in a single operation. Trying to conduct this reaction using a molar ratio of BDCB to BQ (2:3) led to a very slight increase of 2%. in the yield of **40**. It was also found that the formation of **40** is greatly affected by dilution of the reaction mixture. We could not detect the formation of **40** on dilution from 1.00 mmol to 0.01 mmol scales of BDCB **17** or **19** in the same amount of solvent. We note that the synthesis of another nonacene derivative containing quinone moieties has recently been published by Bunz et al.[78]

Furthermore, the cycloaddition reaction of BDCB **19** or **20** with NQ (**30**) afforded similarly the cyclobuta[*b*]tetracene-1,5,10(2H)-trione **41** (Scheme 9). **41** was characterized spectroscopically. Its IR spectrum showed two characteristic bands at $\tilde{\nu}$ = 1738, 1672 cm^{-1} for C=O stretching vibrations. The ^1H NMR spectrum showed two distinct singlet signals for methoxy protons at δ = 4.00, 4.10 ppm, a singlet at δ = 5.01 ppm (2H) for methylene protons, and a set of peaks for the aryl protons at their expected chemical shifts. Also, the ^{13}C NMR spectrum fits well with the constitution of **41** and displays three characteristic peaks at δ = 182.1, 182.87, 182.94 ppm for the three C=O groups.

The formation of **40** can be rationalized by a tandem reaction involving firstly the bis-cycloaddition reaction of two equivalents of *o*-xylylene intermediate **33** to either double bonds of BQ (**25**) to form diol **37**, which subsequently under-

Photophysical properties

The UV-VIS absorption spectra of compounds **26**, **27**, **32**, **36**, **40** and **41** in THF at of 10 μM concentration are shown in Figure 5,

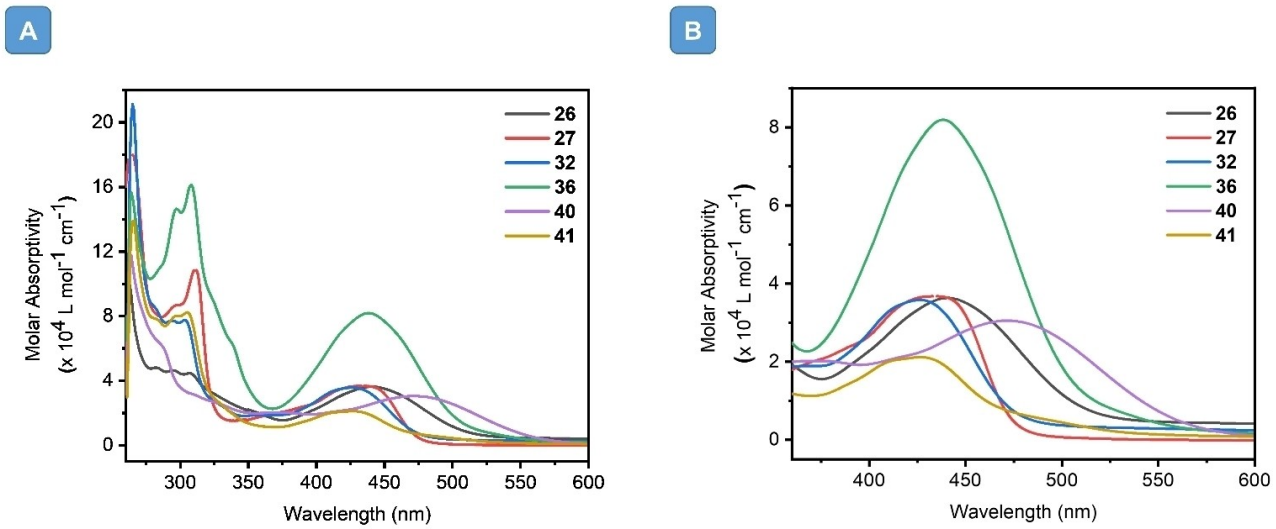

Figure 5. A) The UV-VIS absorption spectra of compounds **26**, **27**, **32**, **36**, **40** and **41** in THF at a concentration of 10 μM. B) onset of the lowest energy band.

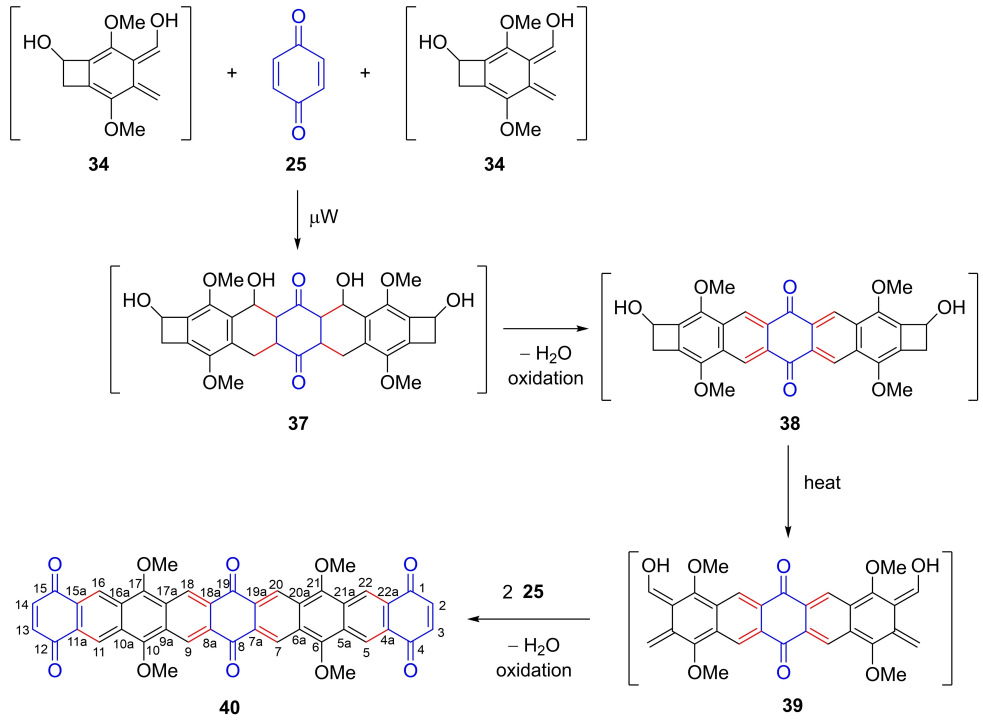

Scheme 8. A plausible mechanism for formation of 6,10,17,21-tetramethoxynonacene-1,4,8,12,15,19-hexaone (**40**). Reaction conditions: **19** or **20** (1.0 mmol), BQ (25) (2.5 mmol), μW, 140 °C, 270 W, 1 h (5 %) or: **19** or **20** (2.0 mmol), BQ (**25**) (3.0 mmol), μW, 140 °C, 270 W, 1 h (7 %).

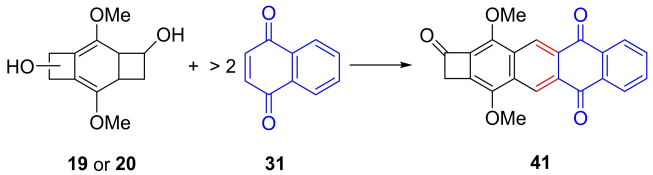

Scheme 9. Synthesis of 3,12-dimethoxycyclobuta[*b*]tetracene-1,5,10(2*H*)-trione (**41**). Reaction conditions: **19** or **20** (1.0 mmol), NQ (**31**) (25 mmol), toluene, 120 °C, sealed tube, 48 h (38 %); or μW, 140 °C, 270 W, 1 h (40 %).

and the data are listed in Table 4. They show a typical behavior of quinone structures with absorption bands at $\lambda = 260$-360 nm for π-π^* transitions and for n-π^* transitions at $\lambda = 400$–450 nm. The lowest energy absorption bands of the tested compounds did not adopt a systematic behavior. The extended nonacene derivative **40** showed the largest red shifted absorption at $\lambda_{max} = 471$ nm while bromotetracenedione **32** and cyclobuta[*b*] tetracenetrione **41** displayed the largest blue shift for each at $\lambda_{max} = 427$ nm. Increasing the number of quinone rings lead to red shifted absorptions; thus, the maximum wavelength of **40** is more than both 1,4-anthraquinone **26** and pentacenetetraone **27**. Surprisingly, the largest lowest energy molar absorptivity was displayed by cyclobuta[*b*]anthracenetrione **36** ($\varepsilon_{max} = 8.6\text{x}10^4$ L·mol^{-1}·cm^{-1}), while the lowest one was that of cyclobuta[*b*]tetracenetrione **41** ($\varepsilon_{max} = 2.3\text{x}10^4$ L mol^{-1} cm^{-1}).

Table 4. Photophysical properties of compounds **26**, **27**, **32**, **36**, **40** and **41**.

	λ_{max} [nm]	ε_{max} [x 10^4 M^{-1}·cm^{-1}][a]	λ_{em} [nm][b]	$\Delta\nu$ [cm^{-1}][c]	Φ_f [%][b]	τ [ns][b]
26	441	3.1	564	4954	< 1	1.79
27	435	3.8	487	2297	< 1	1.46
32	427	3.4	578	6118	< 1	1.42
36	438	8.6	479	1954	< 1	3.56
40	471	3.4	475	179	3.6	4.14
41	427	2.3	602	6808	< 1	2.08

[a] Molar absorptivity measured in THF at 10 μM concentration. [b] Fluorescence measurements (fluorescence quantum yield Φ_f and lifetime τ) in THF at 10 μM concentration; quantum yield Φ_f. [c] Stoke's shift $\Delta\nu$ [cm^{-1}] = [(1/λ_{abs})-(1/λ_{em})] × 10^7.

The fluorescence emission spectra are depicted in Figure 6A. The unfitted fluorescence decay curves are shown in Figure 6B. The fluorescence spectra were measured in THF at a concentration of 1×10^{-6} M. The data shown in Table 6 allow to distinguish between bromine containing compounds **26**, **27** and **32** on the one hand and compounds **36**, **40**, and **41** on the other hand. The known quenching effect of bromine substituents[79] is reflected by the significantly shorter fluorescence life times of the first three compounds as compared to those of the second group. The presence of bromo substituents in **26**, **27** and **32** induces a clear heavy atom effect that decreases the fluorescence by increasing the intersystem crossing (ISC).[80–82] While there are some reports concerning the use of 9,10-anthraquinones in the context of organic light-emitting diodes (OLEDs) through thermally activated delayed fluorescence (TADF),[83–86] fluorescence properties 1,4-anthraquinones such as **26** have much less been investigated.[87–90] A derivative of 2,9-dibromopentacene-6,13-

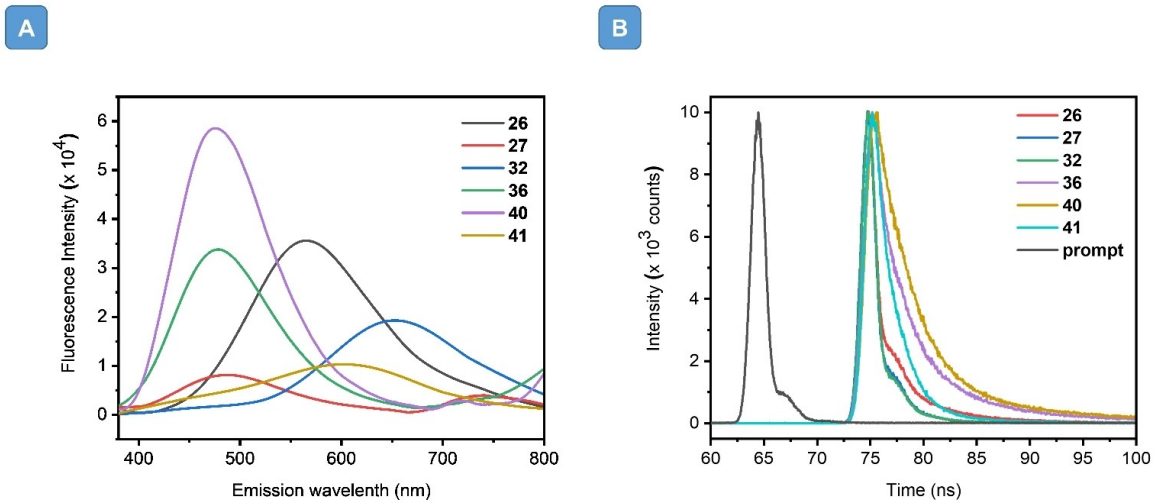

Figure 6. A) The fluorescence emission spectra of compounds **26**, **27**, **32**, **36**, **40** and **41** at a concentration of 1 μM in THF. B) The unfitted fluorescence decay curves of the same compounds

Table 5. Cyclovoltammetry[a] data of compounds **26**, **27**, **32** and **40**.

	E_{pa} [V]	E_{pc} [V]	ΔE [V][b]	$E_{1/2}$ [V][c]	E_{HOMO} [eV][d]	E_{LUMO} [eV][d]	ΔE_{redox} [eV][d]
26	−1.11	−1.80	0.69	−1.46	−6.03	−3.30	2.73
	−1.64	−2.31	0.71	−1.98			
27	−0.80	−1.57	0.77	−1.19	−6.00	−3.10	2.90
	−1.29	−1.84	0.55	−1.57			
32	−0.65	−1.63	0.92	−1.14	−5.99	−3.30	2.69
	−1.46	−2.37	0.91	−1.92			
40	−1.39	−1.52	0.13	−1.49	−6.29	−3.41	2.88
	−1.83	−1.97	0.14	−1.90			
	−2.07	−2.20	0.13	−2.14			

[a] Cyclovoltammetry in a 0.1 M solution of Bu_4N^+ PF_6^- in THF at 100 mV s^{-1} scan rate versus FcH/FcH^+ as an internal reference at 25 °C. [b] ΔE (V) = $E_{pa}{}^n$-$E_{pc}{}^n$ (n = 1, 2, 3). [c] Half-wave potential $E_{1/2}$ [V] = ($E_{pa}{}^n$ + $E_{pc}{}^n$)/2. [d] E_{HOMO} = −(4.8-E_{ox}^{onset}) eV, E_{LUMO} = −(4.8 + E_{red}^{onset}) eV, ΔE_{redox} = E_{LUMO}-E_{HOMO}.[99]

Table 6. DFT-calculated HOMO and LUMO energies and optical energy gaps of compounds **26**, **27**, **32**, **36**, **40**, **41**.

	E_{HOMO} [eV][a]	E_{LUMO} [eV][a]	ΔE [eV][a]	ΔE_{opt} [eV][b]
26	−5.72	−3.59	2.13	2.39
27	−6.10	−2.89	3.21	2.60
32	−6.17	−3.05	3.12	2.60
36	−6.11	−3.43	2.68	2.43
40	−6.16	−3.60	2.56	2.18
41	−6.02	−3.08	2.94	2.56

[a] Theoretical HOMO, LUMO energies and energy gap calculated from DFT [B3LYP/6-31++(*d*,*p*)]. [b] optical energy gap ΔE_{opt} [eV] = 1240/λ_{onset}.[101]

dione **27** could further be functionalized and investigated for the application as molecular wires.[91] The data for the cyclobutanone-anellated compounds **36** and **41**, the latter being the benzo anellated homologue of **36**, do not differ significantly, which may possibly be due to the quinone moiety separating the benzoid π systems in **41** in a cross-conjugated way. The compound with the by far largest π system, nonacene **40**, shows the strongest fluorescence at λ_{em} = 475 nm with the highest fluorescence intensity, the lowest Stokes shift ($\Delta\nu$ = 179 cm^{-1}), the largest quantum yield (Φ_f = 3.6 %), and the longest fluorescence lifetime (τ = 4.14 ns) in the series. All other compounds have lower quantum yields (Φ_f < 1 %). This could partly be attributed to the presence of methoxy groups causing efficient intramolecular charge transfer (ICT) to the aromatic rings in the excited state.[92–95] The fluorescence lifetime values of all compounds are small (τ = 1.42-3.65 ns) which is in accord with the efficient non-radiative ICT processes. In addition, large Stokes shifts in the range of 5000–7000 cm^{-1} were displayed by all compounds except **40**. This could be attributed to efficient ICT and structural relaxation in the excited state.[96–98]

Electrochemical characterization

The study of the electrochemical redox behavior was limited herein to the extended quinones anthraquinone **26**, pentacenedione **27**, tetracenedione **32**, and nonacenehexaone **40** in order to avoid the interfering redox behavior of cyclobutenone rings in **36** and **41**. While the first three compounds bear bromo substituents and are less symmetric, nonacenehexaone **40** is a highly symmetric compound. The cyclic voltammograms of anthraquinone **26**, pentacenedione **27**, and tetracenedione **32** (see SI) show two oxidation waves and two reduction waves lacking clear reversibility. In contrast, the cyclic voltammogram of nonacenehexaone **40** (Figure 7) displays three quasi-reversible redox waves. Examining the oxidation potentials (Table 5) of the first anodic process and the first reduction wave potentials of the studied compounds shows that the order of these compounds with respect to their ease of oxidation is **40** > **26** ≈ **27** > **32** reflecting the extended π system in **40**. In addition, Table 5 presents the HOMO and LUMO energies as calculated from the CV data.[99]

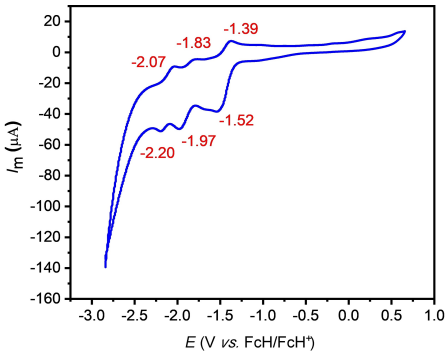

Figure 7. Cyclic voltammogram of nonacenehexaone **40**.

DFT calculations

The DFT calculations were performed using the Gaussian 16 program[100] at B3LYP/6-31++(*d*,*p*) level of theory in order to get some insight into the geometry and the electronic structures of the synthesized compounds. Geometry optimization was performed in the gas phase. The optimized structures of compounds **26**, **27b**, **32**, **36**, **40** and **41** showed all planarity over the region of the extended aromatic systems in addition to the bond lengths with an average of 1.4±0.01 Å and bond angles of about 120±2°. Distortions from these values occur in quinone or cyclobutenone moieties. For comparison, the calculated HOMO and LUMO orbitals of the compounds are depicted in Figure 8, and the relevant numerical values can be found in Table 6. Inspection of the HOMO and LUMO distributions of the quinones reveals that HOMO orbitals are mainly located at electron-rich aromatic rings and away from the quinone rings while the LUMO orbitals are preferentially located at the quinone rings. The calculated energies correspond well to those obtained from the CV measurements. Among the bromine free derivatives the most highly extended π system **40** shows the smallest HOMO-LUMO gap while the opposite is the case for the bromine containing **27** as compared to **26** and **28**. While the HOMO energies of **27** and **40** are quite similar, the main difference lies in their LUMO energies. While the LUMO of **27** shows the largest coefficients at the central quinone moiety, this is the case for the two terminal quinone moieties in **40**.

Conclusion

In conclusion, it has been shown that benzocyclobutenes as well as benzodicyclobutenes serve as useful building blocks for the syntheses of a number of π-extended acenes and cyclobutaacenes by reactions with quinones followed by water elimination and oxidation. The possibility of benzodicyclobutenes and of benzoquinone to react in a bidirectional way makes the approach particularly attractive as shown by the synthesis of a nonacene derivative incorporating three quinone subunits. The compounds obtained were characterized spectroscopically and were investigated by cyclovoltammetry, fluorescence spectroscopy as well as by DFT calculations. Further investigations will head at higher yielding syntheses as well as towards possible applications of these compounds.

Experimental Section

General: Solvents were dried and distilled before use. Toluene and THF were distilled from sodium wire/benzophenone under argon prior to their use, while petroleum ether (PE), dichloromethane (DCM) *tert*-butyl methyl ether (TBME), and ethyl acetate were dried with calcium chloride. Absolute EtOH was supplied by Sigma-Aldrich and used as received.

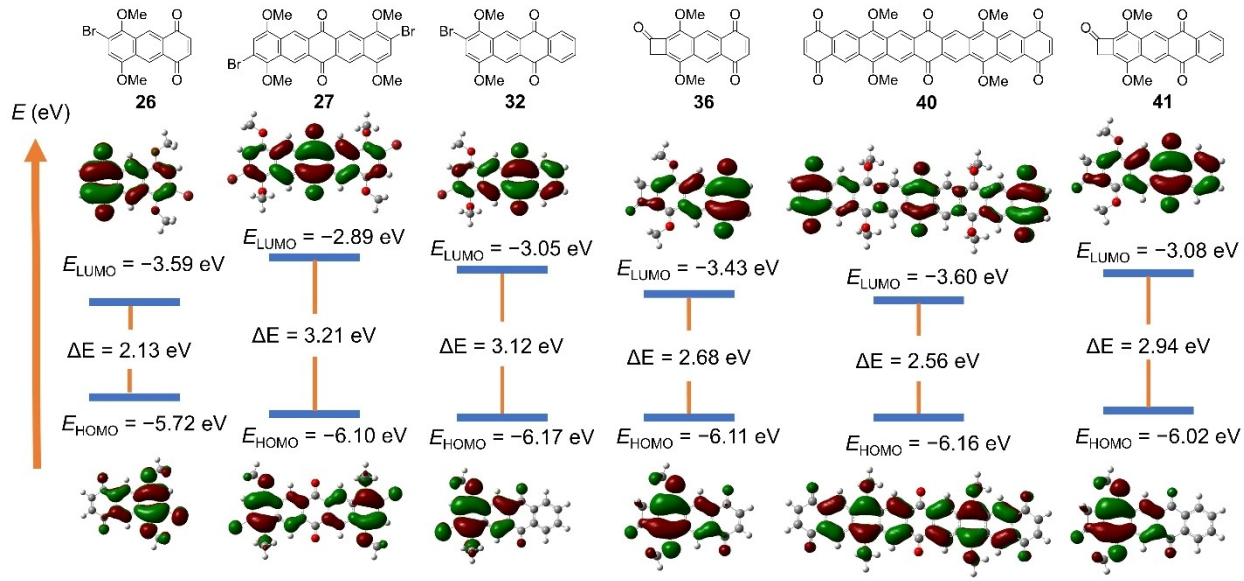

Figure 8. The HOMO and LUMO energy diagram of compounds **26**, **27**, **32**, **36**, **40**, **41**. [DFT, B3LYP/6-31++(*d*,*p*)].

Analytical TLC was performed with Merck 60F-254 silica gel thin layer plates. *Column chromatography* was carried out using silica gel (Macherey-Nagel, 40–63 μm, Silica M) as the stationary phase and indicated eluents by flash chromatography.[102] *Melting points*: Electrothermal IA 9200 Series Digital Melting Point Apparatus. *IR*: Shimadzu IRAffinity-1S with quest ATR unit (32 scans). Intensity of signals are determined as s = strong, m = middle, w = weak, br = broad. *NMR*: Bruker AVS 400 (^{1}H: 400.1 MHz, ^{13}C: 100.6 MHz) and AVS 500 (^{1}H: 500 MHz, ^{13}C: 125.7 MHz) instruments. Chemical shifts δ refer to $\delta_{TMS} = 0.00$ ppm or to residual solvent signals. The multiplicities of the signals were determined by ATP measurements and specified as CH_3, CH, CH_2 or C. Assignment of the ^{13}C signals was made based on 2D NMR spectra (HSQC, HMBC) and in comparison to calculated ^{13}C chemical shifts (ChemDraw® 20.1.0.110). *LC–MS (ESI):* Micromass LCT premier spectrometer with lock-spray unit (ESI), loop mode, HPLC Alliance 2695 column (Waters). Matrix-assisted laser desorption/ionization (MALDI): 5800 MALDI TOF/TOF (ABSciex) using 4-Chloro-α-cyanocinnamic acid (CHCA) as a matrix. *HRMS*: VG-Autospec or Micromass LCT spectrometer with direct insertion probe; 70 eV electron energy and 250 °C source temperature. *UV/VIS spectra* were recorded with a Horiba Dual-FL spectrometer. All samples were diluted with THF and measured in quartz cuvettes with a path length of 1 cm. *Fluorescence spectra* were measured in dilute solutions in 1 cm quartz cuvettes from Hellma Analytics employing a Horiba Fluoromax-4 spectrometer with excitation at the absorption maximum. *Fluorescence quantum yields* were measured in a Horiba Dual-FL instrument with a Horiba Quanta-Phi integrating sphere with an excitation wavelength of 375 nm by comparison of the area below the scattered excitation peak and the emission peak for pure solvent and sample. *Fluorescence lifetimes* were measured by time correlated single photon counting using a Horiba Fluoromax-4 coupled with a Fluorohub and a NanoLED with 370 nm wavelength, pulse width of 1.2 ns and 1 MHz repetition rate. *Cyclovoltammetry* (CV) measurements were carried out with a Gamry Reference 600 Potentiostat/Galvanostat/ZRA. 0.01 mM of the sample compound in freshly distilled THF, and tetrabutylammonium phosphate (TBAP, 0.387 g, 98% purity) was added corresponding to a concentration of 0.1 M. The reference electrode was a Ag/Ag^+ ($AgNO_3$) electrode in acetonitrile with 0.01 M $AgNO_3$ and 0.1 M of TBAP. A 0.25 mm and a 0.1 mm thick platinum wire served as counter and working electrodes, respectively. The scan rate was 100 mV/s. Freshly sublimed ferrocene (FcH) was used for calibration; potentials refer to the FcH/FcH^+ redox couple.

General procedure 1 (GP1) for the synthesis of 18, 19 and 20: Sodium borohydride was added to a solution of aromatic ketones (**15**, **16** or **17**) (10 mmol) in ethanol (30 mL), and the solution was stirred at 25 °C for 30 min. The resulting solution was treated with aq. HCl (1%, v/v, 100 mL) and then extracted with chloroform (3 × 50 mL). The collected organic layers were washed with aq. $NaHCO_3$ (0.1 M, 100 mL), brine and water and dried over anhydrous $MgSO_4$. The solvent was removed at reduced pressure to give practically pure product.

4-Bromo-2,5-dimethoxybicyclo[4.2.0]octa-1(6),2,4-trien-7-ol (18): GP1, bicyclo[4.2.0]octa-1(6),2,4-trien-7-one (**15**) (2560 mg, 10 mmol), sodium borohydride (1141 mg, 30 mmol). The obtained product was recrystallized from TBME/PE (1:5, v/v) to give **18** (1935 mg, 7.5 mmol, 75%) as colorless crystals [R_f = 0.72 ($CHCl_3$/acetone 4:1), m. p. 108–110 °C].

One-step synthesis of 18 starting from 1,4-dibromo-2,5-dimethoxybenzene (12): Under argon THF (20 mL) was added to a 100 mL flamed-dried Schlenk tube A. The tube was inserted into an ice bath and the temperature decreased to 0 °C before butyllithium (2.4 mL, 2.5 M in hexane, 6 mmol, 1.5 equiv) was added dropwise with continuous stirring. Upon completion, the system was allowed to reach room temperature (25 °C) and kept at this temperature for 24 h. Meanwhile, under argon another Schlenk tube B was charged with TMP (0.68 mL, 4.0 mmol, 1.0 equiv) and THF (10 mL) and then cooled to 0 °C. Butyllithium (1.6 mL, 2.5 M in hexane, 4.0 mmol, 1.0 equiv) was added dropwise with stirring, and the mixture was maintained at this temperature for 0.5 h. Schlenk tube A was cooled to 78 °C in an acetone-dry ice bath. 1,4-Dibromo-2,5-dimethoxybenzene (**12**, 1184 mg, 4 mmol, 1.0 equiv) in THF (5 mL) was added dropwise. Afterwards, the content of tube B (LiTMP solution) was added dropwise. After the reaction finished as monitored by TLC, saturated aqueous NH_4Cl (10 mL) was added. The mixture was slowly warmed to 25 °C. The crude mixture was diluted with water (30 mL) and then extracted with DCM (3 x 50 mL). The combined organic layer were washed with brine (50 mL) and dried with $MgSO_4$. The solvent was evaporated at reduced pressure and purified by recrystallization from TBME/PE (1:5, v/v) to give **18** (630 mg, 2.4 mmol, 61%) as colorless crystals [R_f = 0.72 ($CHCl_3$/acetone 4:1), m. p. 108–110 °C].

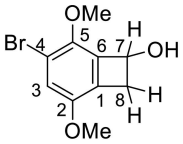

18

IR (neat): $\tilde{\nu}$ = 3201 (br, m, OH), 2936 (w), 2344 (w), 1488 (s), 1418 (s), 1383 (m), 1339 (m), 1244 (s), 1159 (m), 1118 (s), 1039 (s), 983 (m), 926 (w), 833 (m), 797 (m), 666 (m) cm^{-1}. ^{1}H NMR ($CDCl_3$, 400 MHz): δ = 2.31 (d, 1H, $J_{OH\text{-}H7}$ = 10.2 Hz, OH), 3.04 (dd, 1H, $^2J_{H8\text{-}H8'}$ = −14.2 Hz, $J_{H8\text{-}H7}$ = 1.8 Hz, H8), 3.66 (dd, 1H, $^2J_{H8'\text{-}H8}$ = −14.2 Hz, $J_{H8'\text{-}H7}$ = 4.6 Hz, H8′), 3.81 (s, 3H, 2-OCH_3), 4.10 (s, 3H, 5-OCH_3), 5.36 (ddd, 1H, $J_{H7\text{-}OH}$ = 10.2 Hz, $J_{H7\text{-}H8}$ = 1.8 Hz, $J_{H7\text{-}H8'}$ = 4.6 Hz, H7), 7.02 (s, 1H, H3) ppm. ^{13}C NMR ($CDCl_3$, 100 MHz): δ = 41.5 (CH_2, C8), 56.5 (CH_3, 2-OCH_3), 58.4 (CH_3, 5-OCH_3), 70.6 (CH, C7), 109.6 (C, C4), 120.4 (CH, C3), 125.9 (C, C1), 131.7 (C, C6), 145.8 (C, C5), 148.8 (C, C2) ppm. MS (70 eV): *m/z* (%) = 260 (43) $[M+2]^+$, 258 (51) $[M]^+$, 245 (76) $[M+2-CH_3]^+$, 243 (100) $[M-CH_3]^+$. HRMS (ESI): Calcd. for $C_{10}H_{11}BrO_3$ $[M]^+$ 257.9892, found 257.9858.

2,7-Dimethoxytricyclo[6.2.0.0^{3,6}]deca-1,3(6),7-triene-4,10-diol (19): GP1, 2,7-dimethoxytricyclo[6.2.0.0^{3,6}]deca-1,3(6),7-triene-4,10-dione (**16**) (2180 mg, 10.0 mmol), sodium borohydride (2282 mg, 60 mmol). **19** was obtained as a diastereomeric mixture (3:2) (1444 mg, 0.65 mmol), pale yellow solid [R_f = 0.63 ($CHCl_3$/acetone 4:1), m.p. 150–152 °C (mixture)].

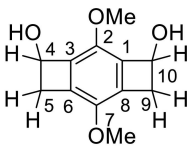

19

IR (neat): $\tilde{\nu}$ = 3259 (br, m, OH), 2919 (m), 2367 (w), 1487 (s), 1415 (s), 1314 (m), 1264 (s), 1199 (m), 1177 (m), 1109 (m), 1067 (m), 1041 (s), 977 (m), 924 (m), 892 (w), 802 (m), 779 (m), 612 (m) cm^{-1}. ^{1}H NMR ($CDCl_3$, 400 MHz): δ = 2.33-2.43 (d, 2H, $J_{OH\text{-}H4}$ = $J_{OH\text{-}H10}$ = 10.2 Hz, 2 OH), 2.98 + 3.21 [dd, 2H, $^2J_{H5\text{-}H5'}$ = $^2J_{H9\text{-}H9'}$ = −14.2 Hz, $J_{H5\text{-}H4}$ = $J_{H9\text{-}H10}$ = 1.8 Hz, H5(9)], 3.54 [dd, 2H, $^2J_{H5'\text{-}H5}$ = $^2J_{H9'\text{-}H9}$ = −14.2 Hz, $J_{H5'\text{-}H4}$ = $J_{H9'\text{-}H10}$ = 1.8 Hz, H5′(9′)], 3.63 + 3.85 (2 s, 3H, 7-OCH_3), 4.01 + 4.05 (2 s, 3H, 2-OCH_3), 5.26 + 5.35 [2ddd, 2H, $J_{H4\text{-}OH}$ = $J_{H10\text{-}OH}$ = 10.2 Hz, $J_{H4\text{-}H5}$ = $J_{H10\text{-}H9}$ = 1.8 Hz, $J_{H4\text{-}H5'}$ = $J_{H10\text{-}H9'}$ = 4.6 Hz, H4(10)] ppm. ^{13}C NMR ($CDCl_3$, 100 MHz): δ = 43.1 [CH_2, C5(9)], 57.3 (CH_3, 7-OCH_3), 57.8 (CH_3, 2-OCH_3), 71.0 [CH, C4(10)], 124.4 [C, C6(8)], 127.5 [C, C1(3)], 128.3 (C, C7), 128.4 (C, C2) ppm. MS (70 eV): *m/z* (%) = 224 (34) $[M+2]^+$, 222

(36) $[M]^+$, 207 (85), 205 (28), 191 (91), 179 (88), 177 (46), 163 (50), 148 (31), 135 (25), 133 (17), 121 (15), 105 (31), 91 (100), 77 (83). HRMS (ESI): calcd. for $C_{12}H_{14}O_4$ $[M]^+$ 222.0892, found 222.0874.

2,7-Dimethoxytricyclo[6.2.0.0^{3,6}]deca-1,3(6),7-triene-4,9-diol (20): GP1, 2,7-dimethoxytricyclo[6.2.0.0^{3,6}]deca-1,3(6),7-triene-4,9-dione (**17**) (2180 mg, 10.0 mmol), sodium borohydride (2282 mg, 60 mmol). After extraction with chloroform the combined extracts were concentrated to one third of its volume. During this time, an insoluble white solid precipitated, was collected and dried under vacuum to give diastereomer **20a** (777 mg, 3.5 mmol, 35%) as a colorless solid [R_f=0.44 ($CHCl_3$/acetone 4:1), m. p: 192–194 °C]. The mother liquor was evaporated under reduced pressure to give diastereomer **20b** (622 mg, 0.3 mmol, 28%) as a pale-yellow solid [R_f=0.51 ($CHCl_3$/acetone 4:1), m. p. 152–154 °C].

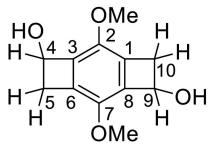

20

20a: IR (neat): $\tilde{\nu}$=3262 (br, m, OH), 2928 (w), 1491 (s), 1422 (s), 1325 (m), 1262 (s), 1202 (w), 1182 (m), 1110 (m), 1073 (m), 1045 (s), 993 (w), 945 (w), 891 (w), 796 (m), 628 (m) cm^{-1}. ^1H NMR ($CDCl_3$, 400 MHz): δ=2.16 (d, 2H, $J_{OH\text{-}H4}=J_{OH\text{-}H9}$ =10.2 Hz, 2 OH), 2.98 [dd, 2H, $J_{H5\text{-}H5'}=J_{H10\text{-}H10'}=-14.2$ Hz, $J_{H5\text{-}H4}=J_{H10\text{-}H9}=1.8$ Hz, H5(10)], 3.59 [dd, 2H, $J_{H5'\text{-}H5}=J_{H10'\text{-}H10}=-14.2$ Hz, $J_{H5'\text{-}H4}=J_{H10'\text{-}H9}=1.8$ Hz, H5′(10′)], 3.97 (s, 6H, 2 OCH_3), 5.27 [ddd, 2H, $J_{H4\text{-}OH}=J_{H9\text{-}OH}=10.2$ Hz, $J_{H4\text{-}H5}=J_{H9\text{-}H10}=1.8$ Hz, $J_{H4\text{-}H5'}=J_{H9\text{-}H10'}=4.6$ Hz, H4(9)] ppm. ^{13}C NMR (acetone-d_6, 100 MHz): δ=39.7 [CH_2, C5(10)], 56.8 (CH_3, OCH_3), 69.1 [CH, C4(9)], 126.5 [C, C1(6)], 134.0 [C, C3(8)], 146.3 [C, C2(7)] ppm. MS (70 eV): *m/z* (%)=222 (66) $[M]^+$, 207 (100) $[M–CH_3]^+$, 192 (10), 179 (13), 177 (17), 164 (19), 147 (23), 121 (13), 91 (43), 77 (38). HRMS (ESI): Calcd. for $C_{12}H_{14}O_4$ $[M]^+$ 222.0892, found 222.0884.

20b: IR (neat): $\tilde{\nu}$=3152 (br, m, OH), 2930, (m), 2359 (w), 1487 (s), 1454 (m), 1424 (m), 1329 (w), 1292 (m), 1261 (s), 1202 (w), 1044 (s), 987 (m), 966 (w), 944 (m), 890 (w), 796 (w), 663 (w) cm^{-1}. ^1H NMR ($CDCl_3$, 400 MHz): δ=2.42 (d, 2H, $J_{OH\text{-}H4}=J_{OH\text{-}H9}$ =10.2 Hz, 2 OH), 2.93 [dd, 2H, $J_{H5\text{-}H5'}=J_{H10\text{-}H10'}=-14.2$ Hz, $J_{H5\text{-}H4}=J_{H10\text{-}H9}=1.8$ Hz, H-5(10)], 3.57 [dd, 2H, $J_{H5'\text{-}H5}=J_{H10'\text{-}H10}=-14.2$ Hz, $J_{H5'\text{-}H4}=J_{H10'\text{-}H9}=$ 1.8 Hz, H5′(10′)], 3.97 (s, 6H, 2 OCH_3), 5.24 [ddd, 2H, $J_{H4\text{-}OH}=J_{H9\text{-}OH}=$ 10.2 Hz, $J_{H4\text{-}H5}=J_{H9\text{-}H10}=1.8$ Hz, $J_{H4\text{-}H5'}=J_{H9\text{-}H10'}=4.6$ Hz, H4(9)] ppm. ^{13}C NMR ($CDCl_3$, 100 MHz): δ=40.7 [CH_2, C5(10)], 57.6 (CH_3, OCH_3), 69.8 [CH_3, C4(9)], 126.7 [C, C1(6)], 133.8 [C, C3(8)], 143.9 [C, C2(7)] ppm. MS (70 eV): *m/z* (%)=224 (19) $[M+2]^+$, 222 (48) $[M]^+$, 207 (81) $[M–CH_3]^+$, 193 (33), 177 (52), 163 (34), 147 (25), 135 (22), 121 (25), 119 (19), 91 (89), 77 (100). HRMS (ESI): Calcd. for $C_{12}H_{14}O_4$ $[M]^+$ 222.0892, found 222.0884.

General Procedure 2 (GP2)

Method A (conventional heating): A mixture of benzocyclobutene derivative **18** or benzodicyclobutene derivatives **19** or **20** and benzoquinone (**25**) or naphthoquinone (**31**) in anhydrous toluene (5 mL) was heated in a sealed pressure tube at 140 °C for 48 h. PE (20 mL) was added to the resulting mixture, which was then filtered at reduced pressure and washed thoroughly with hot MeOH (3× 20 mL). The combined organic filtrates were evaporated at reduced pressure and then purified by column chromatography.

Method B (microwave heating): A mixture of benzocyclobutene derivative **18** or benzodicyclobutene derivatives **19** or **20** and benzoquinone (**25**) or naphthoquinone (**31**) in anhydrous toluene (2 mL) was placed in a microwave vessel, flushed with argon and then subjected to microwave irradiation (60 min, 120 °C, 200 W). PE (20 mL) was added to the resulting mixture, which was then filtered at reduced pressure and washed thoroughly with hot MeOH (3× 20 mL). The combined organic filtrates were evaporated at reduced pressure and then purified by column chromatography.

6-Bromo-5,8-dimethoxyanthracene-1,4-dione (26) and 2,9-dibromo-1,4,8,11-tetramethoxypentacene-6,13-dione (27): GP 2, *Method A*. Benzocyclobutenol **18** (260 mg, 1.0 mmol), benzoquinone (**25**) (500 mg, 4.6 mmol). Column chromatography (TBME/PE 1:3) gave pure **26** (132 mg, 0.4 mmol, 38%) as red crystals [R_f=0.52 (TBME/PE 1:3), m. p. 214-216 °C.]. The insoluble part in MeOH was recrystallized from hot DMSO to give an orange solid which is filtered at reduced pressure, washed thoroughly with MeOH, dried at reduced pressure overnight to afford **27** (128 mg, 0.22 mmol, 22%); orange solid [R_f=0.30 ($CHCl_3$/PE 1:3), m. p. >300 °C].

Method B: Benzocyclobutenol **18** (260 mg, 1.0 mmol), benzoquinone (**25**) (500 mg, 4.6 mmol). Column chromatography (TBME/PE 1:3) gave pure **26** (180 mg, 0.5 mmol, 52%) as red crystals [R_f=0.52 (TBME/PE 1:3), m. p. 214-216 °C.]. The insoluble part in MeOH was recrystallized from hot DMSO to give an orange solid which is filtered off, washed thoroughly with MeOH, dried at reduced pressure overnight to afford **27** (152 mg, 0.3 mmol, 26%); orange solid [R_f=0.30 ($CHCl_3$/PE 1:3), m. p. >300 °C].

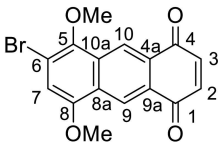

26

26: IR (neat): $\tilde{\nu}$=2918 (w), 1715 (w), 1671 (m), 1598 (m), 1576 (m), 1462 (m), 1432 (m), 1375 (m), 1323 (m), 1297 (s), 1209 (m), 1149 (m), 1116 (m), 1055 (m), 1008 (m), 949 (m), 928 (w), 845 (s), 802 (m), 773 (w), 727 (m), 705 (m) cm^{-1}. ^1H NMR ($CDCl_3$, 400 MHz): δ=4.03 (s, 3H, OCH_3), 4.05 (s, 3H, OCH_3), 7.09 (s, 1H, H7), 7.10 (s, 2H, H2, H3), 8.80 (s, 1H, H9), 9.00 (s, 1H, H10) ppm. ^{13}C NMR ($CDCl_3$, 100 MHz): δ=56.2 (CH_3, 8-OCH_3), 62.1 (CH_3, 5-OCH_3), 111.9 (CH, C7), 117.1 (C, C6), 122.8 (C, C10), 124.2 (CH, C9), 127.1 (C, C10a), 128.0 (C, C9a), 129.5 (C, C4a), 130.6 (C, C8a), 140.0 (CH, C3), 140.1 (CH, C2), 148.5 (C, C5), 153.6 (C, C8), 184.3 (C, 4-C=O), 184.5 (C, 1-C=O) ppm. UV/Vis (THF): λ_{max} (ε)=441 (31.5), 307 (38.0), 295 (39.0), 283 (40.6) nm (mM^{-1} cm^{-1}). Fluorescence (THF): λ_{ex}=268 nm; λ_{em}=564 nm. MS (70 eV): *m/z* (%)=348 (31) $[M+2]^+$, 346 (35) $[M]^+$, 333 (99) $[M+2–CH_3]^+$, 331 (100) $[M–CH_3]^+$, 305 (11), 307 (12). HRMS (ESI): Calcd. for $C_{16}H_{11}BrO_4$ $[M]^+$ 345.9841, found 345.9831.

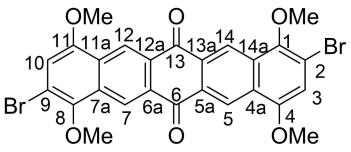

27

27: IR (neat): $\tilde{\nu}$=2937 (w), 1673, (s), 1597 (s), 1457 (m), 1429 (m), 1410 (m), 1381 (m), 1318 (s), 1268 (s), 1231 (m), 1136 (s),1024 (s), 975 (m), 952 (s), 935 (s), 830 (s), 796 (s), 745 (s), 720 (s) cm^{-1}. ^1H NMR ($CDCl_3$, 400 MHz): δ=4.00 [s, 6H, 1(8)-OCH_3], 4.10 [s, 6H, 4(11)-OCH_3], 7.42 [s, 2H, H3(10)], 8,87 [s, 2H, H5(12)], 9.05 [s, 2H, H7(14)] ppm. UV/Vis (THF): λ_{max} (ε)=435 (38.3), 313 (185.5), 267 (113.7) nm (mM^{-1} cm^{-1}). Fluorescence (THF): λ_{ex}=269 nm; λ_{em}=487 nm. MS (70 eV): *m/z* (%)=588 (28) [M, 2 $^{81}Br]^+$, 586 (56) [M, ^{81}Br, $^{79}Br]^+$, 584 (28) [M, 2 $^{79}Br]^+$, 573 (14) $[M+4–CH_3]^+$, 571 (28) $[M+2–CH_3]^+$, 569 (14) $[M–CH_3]^+$. HRMS (ESI): Calcd. for $C_{26}H_{18}Br_2O_6$ $[M]^+$ 583.9470, found 583.9431.

2,9-dibromo-1,4,8,11-tetramethoxypentacene-6,13-diol (28): A mixture of **27** (10.0 mg, 0.017 mmol) and a large excess of $NaBH_4$ (8.0 mg, 0.211 mmol) was heated in MeOH (10 mL) for 3 h. The solution was then treated with 0.1 N HCl (10 mL), diluted with distilled water (20 mL) and extracted with chloroform (2×15 mL). The combined organic extracts were washed with $NaHCO_3$ solution (0.2 N, 10 mL), brine and then water followed by drying over $MgSO_4$. The organic solvent was removed at reduced pressure and dried under vacuum to obtain analytically pure compound **28** (3.8 mg, 0.006 mmol, 38%) as a yellow solid (m. p. >300 °C), which deepens in color on standing and in $CDCl_3$ during NMR measurement forming **27**.

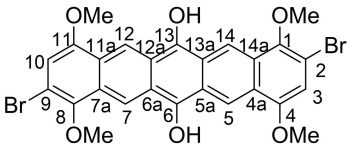

28

^{1}H NMR ($CDCl_3$, 400 MHz): δ = 4.09 (s, 12H, 4 OCH_3), 7.09 [s, 2H, H3(10)], 9.11 [s, 2H, H5(12)], 9.29 [s, 2H, H7(14)] ppm. ^{13}C NMR [d_6-DMSO/$CDCl_3$ (1:1), 500 MHz]: δ = 56.1 (CH_3, 4,11-OCH_3), 60.2 (CH_3, 1,8-OCH_3), 111.8 [CH, C3(10)], 112.7 [C, C2(9)], 117.1 [C, C4a(11a)], 123.6 [CH, C7(14)], 125.1 [CH, C5(12)], 127.6 [C, C5a(12a)], 130.9 [C, C6a(13a)], 131.4 [+, C7a(14a)], 140.7 [+,C1(8)], 148.2 [+, C4(11)], 153.6 [+, C6(13)] ppm. HRMS (ESI): Calcd. for $C_{26}H_{22}Br_2NaO_6$ [M + 2H + Na]$^+$ 610.9681, found 610.9761.

8-Bromo-7,10-dimethoxytetracene-5,12-dione (32): GP2. Benzocyclobutenol **18** (260 mg, 1.0 mmol), naphthoquinone (**31**) (727 mg, 4.6 mmol). The reaction mixture was directly subjected to chromatographic purification (PE/TBME 3:1) to give pure **32** (Method A: 186 mg, 0.5 mmol, 47%. Method B: 230 mg, 0.6 mmol, 58%), dark orange solid [R_f = 0.60 (TBME/PE 1:3), m. p. 244–246 °C].

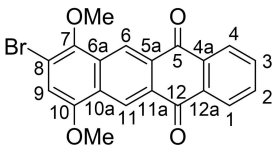

32

IR (neat): $\tilde{\nu}$ = 2941 (m), 1672 (s), 1591 (s), 1463 (m), 1431 (m), 1415 (m), 1380 (m), 1324 (s), 1278 (s), 1242 (m), 1140 (m), 1100 (m), 1052 (m), 975 (m), 950 (s), 929 (m), 854 (m), 841 (m), 797 (m), 711 (s), 672 (m), 633 (w), 611 (w) cm^{-1}. ^{1}H NMR ($CDCl_3$, 400 MHz): δ = 4.05 (s, 3H, 10-OCH_3), 4.06 (s, 3H, 7-OCH_3), 7.06 (s, 1H, H9), 7.83-7.86 (m, 2H, H2, H3), 8.40-8.42 (m, 2H, H1, H4), 9.02 (s, 1H, H11), 9.20 (s, 1H, H6) ppm. ^{13}C NMR ($CDCl_3$, 100 MHz): δ = 56.2 (CH_3, 10-OCH_3), 62.2 (CH_3, 7-OCH_3), 111.6 (CH, C9), 118.3 (C, C8), 123.5 (CH, C6), 124.9 (CH, C11), 127.50 (+, C6a), 127.53 (CH, C1), 127.55 (CH, C4), 129.4 (C, C11a), 130.91 (C, C5a), 130.93 (C, C10a), 134.16 (C, C3), 134.26 (C, C2), 134.34 (C, C4a), 134.42 (C, C12a), 148.4 (C, C7) 153.6 (C, C10), 182.5 (C, C12), 182.8 (C, C5) ppm. UV/Vis (THF): λ_{max} (ε) = 427 (34.4), 303 (74.7), 293 (74.1), 294 (74.7) nm (mM^{-1} cm^{-1}). Fluorescence (THF): λ_{ex} = 268 nm; λ_{em} = 578, 776 nm. MS (70 eV): *m/z* (%) = 398 (11) [M + 2]$^+$, 396 (11) [M]$^+$, 383 (30) [M + 2–CH_3]$^+$, 381 (30) [M–CH_3]$^+$, 322 (17), 219 (38), 131 (30), 111 (38), 97 (70), 83 (66), 71 (100). HRMS (EI): Calcd. for $C_{20}H_{13}BrO_4$ [M]$^+$ 395.9997, found 396.0025.

3,10-Dimethoxycyclobuta[*b*]anthracene-1,5,8(2*H*)-trione (36) and 6,10,17,21-Tetramethoxynonacene-1,4,8,12,15,19-hexaone (40): GP2, benzodicyclobutene derivative **19** or **20** (224 mg, 1 mmol), benzoquinone (**25**) (270 mg, 2.5 mmol). Direct column chromatography of the reaction mixture (TBME/PE 1:6) gave **36** (Method A: 105 mg, 0.34 mmol, 34%; method B: 126 mg, 0.41 mmol, 41%); deep red solid, R_f = 0.68 ($CHCl_3$), m. p. 242–244 °C] and **40** (only method B: 34 mg, 0.05 mmol, 5%. Bluish red solid (34 mg, 0.05 mmol, 5%), R_f = 0.56 ($CHCl_3$), m. p. 274–276 °C].

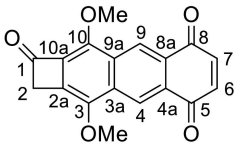

36

36:. IR (neat): $\tilde{\nu}$ = 2954 (w), 2362 (w), 2086 (w), 2018 (w), 1665 (s), 1596 (s), 1449 (m), 1427 (m), 1374 (m), 1323 (m), 1294 (s), 1145 (s), 1074 (s), 994 (s), 931 (m), 850 (s), 778 (w), 737(m), 704 (m), 653 (m) cm^{-1}. ^{1}H NMR ($CDCl_3$, 400 MHz): δ = 3.97 (s, 3H, 3-OCH_3), 4.07 (s, 3H, 10-OCH_3), 5.00 (s, 2H, H2), 7.12 (s, 2H, H6, H7), 8.85 (s, 2H, H4, H9) ppm. ^{13}C NMR ($CDCl_3$, 100 MHz): δ = 57.4 (CH_2, C2), 62.2 (CH_3, 3-OCH_3), 64.4 (CH_3, 10-OCH_3), 123.6 (CH, C4), 124.0 (CH, C9), 128.1 (C, C2a), 128.7 (C, C10a), 128.7 (C, C3a), 130.2 (C, C8a), 132.1 (C, C9a), 133.5 (C, C4a), 140.1 (CH, C6), 140.1 (CH, C7), 152.4 (C, C3), 152.9 (C, C10), 183.8 (C, C5), 184.6 (C, C8), 184.6 (C, C1) ppm. UV/Vis (THF): λ_{max} (ε) = 438 (85.7), 308 (154.3), 297 (144.4), 267 (135.4) nm (mM^{-1} cm^{-1}). Fluorescence (THF): λ_{ex} = 268 nm; λ_{em} = 479 nm. MS (70 eV): *m/z* (%) = 310 (88) [M + 2]$^+$, 295 (100) [(M + 2)-CH_3]$^+$, 280 (68) [(M + 2)-2CH_3]$^+$. HRMS (EI): Calcd. for $C_{18}H_{12}O_5$ [M + 2H]$^+$ 310.0841, found 310.0841.

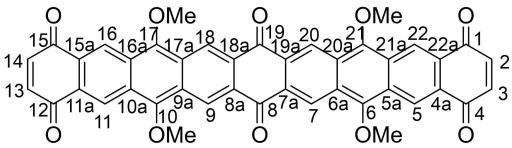

40

40: IR (neat): $\tilde{\nu}$ = 2922 (s), 2851 (s), 1665 (s), 1614 (m), 1472 (m), 1456 (m), 1439 (m), 1387 (m), 1302 (s), 1273 (s), 1215 (m), 1148 (m), 1167 (w), 1117 (m), 1086 (m), 964 (w), 849 (m), 822 (m), 758 (s) cm^{-1}. ^{1}H NMR ($CDCl_3$, 400 MHz): δ 4.02 (s, 12H, 4 OCH_3), 6.92 [s, 4H, H2(3,13,14)], 7.08 [s, 4H, H7(9,18,20)], 9.02 [s, 4H, (H5(11,16,22)] ppm. ^{13}C NMR ($CDCl_3$, 100 MHz): δ 55.9 (CH_3, 4 OCH_3), 107.5 [CH, C7(9,18,C20)], 123.5 [CH, C5(11,16,22)], 127.6 [C, C6a(9a,17a,20a)], 128.1 [C, C5a(10a,16a,21a)], 130.7 [C, C4a(11a,15a,22a)], 135.2 [C,C7a (8a,18a,19a)], 140.0 [CH, C2(3,13,14)], 150.9 [C, C6(10,17,20)], 173.6 [C, C8(19)], 184.81 [C, C1(4,12,15)] ppm. UV/Vis (THF): λ_{max} (ε) = 471 (98.4), 268 (33.4) nm (mM^{-1} cm^{-1}). Fluorescence (THF): λ_{ex} = 268 nm; λ_{em} = 475 nm. LC–MS (ESI, 70 eV): *m/z* (%) = 1348 (11) [2(M + H-C_2H_2) + Na], 686 (48) [M + H + Na–C_2H_2], 685 (100) [M + Na–C_2H_2], 663 (10) [M + Na–C_2H_2–CH_3]. MALDI-TOF: *m/z* = 688 [M]$^+$. HRMS (EI): Calcd. for $C_{40}H_{23}O_{10}$ [M + H–C_2H_2] 663.1280, found 663.4554. Calcd. for $C_{30}H_{22}O_4$ [M + 6H–6CO–2 C_2H_2–2CH_3]$^+$ 446.1518, found 446.1543.

3,12-Dimethoxycyclobuta[*b*]tetracene-1,5,10(2*H*)-trione (41): GP2, benzodicyclobutene **19** or **20** (224 mg, 1 mmol), naphthoquinone (**31**) (395 mg, 2.5 mmol), column chromatography (TBME/PE 1:3) gave **41** (method A: 136 mg, 0.38 mmol, 38%; method B: 143 mg, 0.40 mmol, 40%) as a brown solid [R_f = 0.71 ($CHCl_3$), m. p. 110–112 °C].

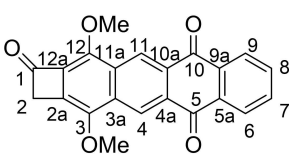

41

IR (neat): $\tilde{\nu}$ = 2922 (s), 2852 (s), 1738 (m), 1672 (m), 1591 (m), 1459 (m), 1379 (m), 1324 (m), 1282 (s), 1212 (m), 1144 (m), 1067 (m), 1003 (s), 968 (m), 923 (m), 797 (m), 715 (s), 614 (w) cm^{-1}. ^1H NMR ($CDCl_3$, 400 MHz): δ = 4.00 (s, 3H, 12-OCH_3), 4.10 (s, 3H, 2-OCH_3), 5.01 (s, 2H, H2), 7.85–7.88 (m, 2H, H7, H8), 8.41–8.44 (m, 2H, H6, H9), 9.08 (s, 2H, H4, H11) ppm. ^{13}C NMR ($CDCl_3$, 100 MHz): δ 57.5 (CH_2, C2), 62.2 (CH_3, 3-OCH_3), 64.5 (CH_3, 12-OCH_3), 124.3 (CH, C4), 124.7 (CH, C11), 127.5 (CH, C6), 127.5 (CH, C9), 129.1 (C, C2a), 129.5 (C, C12a), 130.2 (C, C10a), 130.6 (C, C3a), 131.8 (C, C11a), 133.4 (C, C4a), 134.2 (CH, C7), 134.2 (CH, C8), 134.5 (C, C5a), 134.5 (C, C9a), 152.3 (C, C3), 152.8 (C, C12), 182.1 (C, C5), 182.87 (C, C10), 182.94 (C, C1) ppm. UV/Vis (THF): λ_{max} (ε) = 427 (23.2), 305 (83.0), 297 (81.5) nm (mM^{-1} cm^{-1}). Fluorescence (THF): λ_{ex} = 267 nm; λ_{em} = 415, 602 nm. MS (70 eV): *m/z* (%) 360 (3) $[M+2]^+$, 347 (9) $[M+2-CH_3]^+$, 329 (81) [M-OCH_3]. HRMS (ESI): Calcd. for $C_{22}H_{14}O$ 360.0998, found 360.0963 $[M+2]^+$; calcd. for $C_{21}H_{13}O_4$ $[M-CH_2=O]^+$ 329.0814, found 329.0788.

Acknowledgements

Both Amr M. Abdelmoniem and Ismail A. Abdelhamid acknowledge the Alexander von Humboldt Foundation for a Georg Forster and an Alexander von Humboldt research fellowship, respectively. We thank Mr. Patrick Bessel, M. Sc., and Mr. Pascal Rusch, M. Sc., Institut für Physikalische Chemie und Elektrochemie, Leibniz Universität Hannover, for their help in measuring UV and fluorescence spectra, respectively. We are indebted to Prof. Dr. Andreas Pich, Medizinische Hochschule Hannover, for performing the MALDI measurement of ***40****. Open Access funding enabled and organized by Projekt DEAL.*

Conflict of Interest

The authors declare no conflict of interest.

Keywords: Benzocyclobutenes · Bidirectional acene synthesis · Cycloaddition · Photophysical properties · Quinones

[1] O. Diels, K. Alder, *Justus Liebigs Ann. Chem.* **1928**, *460*, 98–122.
[2] O. Diels, K. Alder, P. Pries, *Ber. Dtsch. Chem. Ges.* **1929**, *62B*, 2081–2087.
[3] M. C. Kloetzel, *Org. React.* **1948**, *4*, 1–59.
[4] H. L. Holmes, *Org. React.* **1948**, *4*, 60–173.
[5] D. Boger, S. Weinreb, *Vol. 47*, 1st ed., **1987**.
[6] J. Sauer, *Angew. Chem.* **1966**, *78*, 233–252; *Angew. Chem. Int. Ed.* **1966**, *5*, 211–230.
[7] J. Sauer, *Angew. Chem.* **1967**, *79*, 76–94; *Angew. Chem. Int. Ed.* **1967**, *6*, 16–33.
[8] Q. Chen, J. Gao, C. Jamieson, J. Liu, M. Ohashi, J. Bai, D. Yan, B. Liu, Y. Che, Y. Wang, K. N. Houk, Y. Hu, *J. Am. Chem. Soc.* **2019**, *141*, 14052–14056.
[9] L. Gao, C. Su, X. Du, R. Wang, S. Chen, Y. Zhou, C. Liu, X. Liu, R. Tian, L. Zhang, K. Xie, S. Chen, Q. Guo, L. Guo, Y. Hano, M. Shimazaki, A. Minami, H. Oikawa, N. Huang, K. N. Houk, L. Huang, J. Dai, X. Lei, *Nat. Chem.* **2020**, *12*, 620–628.
[10] M. Juhl, D. Tanner, *Chem. Soc. Rev.* **2009**, *38*, 2983–2992.
[11] K. C. Nicolaou, S. A. Snyder, T. Montagnon, G. Vassilikogiannakis, *Angew. Chem.* **2002**, *114*, 1742–1773; *Angew. Chem. Int. Ed.* **2002**, *41*, 1668–1698.
[12] S. P. Ross, T. R. Hoye, *Nat. Chem.* **2017**, *9*, 523–530.
[13] S. Kotha, N. N. Rao, O. Ravikumar, G. Sreevani, *Tetrahedron Lett.* **2017**, *58*, 1283–1286.
[14] H. Lv, L. You, S. Ye, *Adv. Synth. Catal.* **2009**, *351*, 2822–2826.
[15] H. Ohara, H. Kiyokane, T. Itoh, *Tetrahedron Lett.* **2002**, *43*, 3041–3044.
[16] M. Potowski, M. Schürmann, H. Preut, A. P. Antonchick, H. Waldmann, *Nat. Chem. Biol.* **2012**, *8*, 428–430.
[17] M. D. Rozeboom, I. M. Tegmo-Larsson, K. N. Houk, *J. Org. Chem.* **1981**, *46*, 2338–2345.
[18] J. Breton, E. Nabedryk, *Biochimica Biophysica Acta* **1996**, *1275*, 84–90.
[19] T. S. Kashey, D. D. Luu, J. C. Cowgill, P. L. Baker, K. E. Redding, *Photosynth. Res.* **2018**, *138*, 1–9.
[20] W. Lubitz, *Pure Appl. Chem.* **2003**, *75*, 1021–1030.
[21] C. Cleren, L. Yang, B. Lorenzo, N. Y. Calingasan, A. Schomer, A. Sireci, E. J. Wille, M. F. Beal, *J. Neurochem.* **2008**, *104*, 1613–1621.
[22] S. Pepe, S. F. Marasco, S. J. Haas, F. L. Sheeran, H. Krum, F. L. Rosenfeldt, *Mitochondrion* **2007**, *7*, S154-S167.
[23] R. Nageswara Rao, M. V. N. K. Talluri, D. D. Shinde, *J. Pharm. Biomed. Anal.* **2008**, *47*, 230–237.
[24] T. C. Rodick, D. R. Seibels, J. R. Babu, K. W. Huggins, G. Ren, S. T. Mathews, *Nutr. Diet. Suppl.* **2018**, *10*, 1–11.
[25] O. Benzakour, *Thromb. Haemostasis* **2008**, *100*, 527–529.
[26] I. Cirilli, P. Orlando, F. Marcheggiani, P. V. Dludla, S. Silvestri, E. Damiani, L. Tiano, *Antioxidants* **2020**, *9*, 1008.
[27] M. Fusaro, G. Iervasi, M. Fusaro, M. C. Mereu, A. Aghi, M. Gallieni, *Clin. Cases Miner. Bone Metab.* **2017**, *14*, 200–206.
[28] M. K. Shea, S. L. Booth, *Curr. Dev. Nutr.* **2019**, *3*, nzz077.
[29] R. Wallin, L. Schurgers, N. Wajih, *Thromb. Res.* **2008**, *122*, 411–417.
[30] A. Abraham, A. J. Kattoor, T. Saldeen, J. L. Mehta, *Crit. Rev. Food Sci. Nutr.v* **2019**, *59*, 2831–2838.
[31] P. Munoz, S. Munne-Bosch, *Trends Plant Sci.* **2019**, *24*, 1040–1051.
[32] L. Zheng, J. Jin, L. Shi, J. Huang, M. Chang, X. Wang, H. Zhang, Q. Jin, *Crit. Rev. Food Sci. Nutr.* **2020**, *60*, 3916–3930.
[33] S. Kandhasamy, N. Arthi, R. P. Arun, R. S. Verma, *Mater. Sci. Eng. C* **2019**, *102*, 773–787.
[34] K. Zhang, D. Chen, K. Ma, X. Wu, H. Hao, S. Jiang, *J. Med. Chem.* **2018**, *61*, 6983–7003.
[35] L. Acuna, S. Hamadat, N. S. Corbalan, F. Gonzalez-Lizarraga, M. dos Santos-Pereira, J. Rocca, J. S. Diaz, E. Del-Bel, D. Papy-Garcia, R. N. Chehin, P. P. Michel, R. Raisman-Vozari, *Cells* **2019**, *8*, 776.
[36] A. G. Granja, F. Carrillo-Salinas, A. Pagani, M. Gomez-Canas, R. Negri, C. Navarrete, M. Mecha, L. Mestre, B. L. Fiebich, I. Cantarero, M. A. Calzado, M. L. Bellido, J. Fernandez-Ruiz, G. Appendino, C. Guaza, E. Munoz, *J. Neuroimmune Pharmacol.* **2012**, *7*, 1002–1016.
[37] K. Kobayashi, S. Nishiumi, M. Nishida, M. Hirai, T. Azuma, H. Yoshida, Y. Mizushina, M. Yoshida, *Med. Chem.* **2011**, *7*, 37–44.
[38] J. Campanini-Salinas, J. Andrades-Lagos, G. G. Rocha, D. Choquesillo-Lazarte, S. B. Dragnic, M. Faundez, P. Alarcon, F. Silva, R. Vidal, E. Salas-Huenuleo, M. Kogan, J. Mella, G. R. Gajardo, D. Vasquez-Velasquez, *Molecules* **2018**, *23*, 1776/1771-1776/1719.
[39] G. Carr, E. R. Derbyshire, E. Caldera, C. R. Currie, J. Clardy, *J. Nat. Prod.* **2012**, *75*, 1806–1809.
[40] M. Iorio, J. Cruz, M. Simone, A. Bernasconi, C. Brunati, M. Sosio, S. Donadio, S. I. Maffioli, *J. Nat. Prod.* **2017**, *80*, 819–827.
[41] I. Sutradhar, M. H. Zaman, *J. Pharm. Biomed. Anal.* **2021**, *197*, 113941.
[42] T. B. Gontijo, R. P. de Freitas, F. S. Emery, L. F. Pedrosa, J. B. Vieira Neto, B. C. Cavalcanti, C. Pessoa, A. King, F. de Moliner, M. Vendrell, E. N. da Silva Jr., *Biochem. Med. Chem. Lett.* **2017**, *27*, 4446–4456.
[43] J.-J. Lu, J.-L. Bao, G.-S. Wu, W.-S. Xu, M.-Q. Huang, X.-P. Chen, Y.-T. Wang, *Anti-Cancer Agents Med. Chem.* **2013**, *13*, 456–463.
[44] P. Morales, D. Vara, M. Goméz-Cañas, M. C. Zúñiga, C. Olea-Azar, P. Goya, J. Fernández-Ruiz, I. Díaz-Laviada, N. Jagerovic, *Eur. J. Med. Chem.* **2013**, *70*, 111–119.
[45] Y. Wang, P. Pigeon, S. Top, J. Sanz Garcia, C. Troufflard, I. Ciofini, M. J. McGlinchey, G. Jaouen, *Angew. Chem.* **2019**, *131*, 8509–8513; *Angew. Chem. Int. Ed.* **2019**, *58*, 8421–8425.
[46] M. B. Thomas, Y. Hu, W. Shan, K. M. Kadish, H. Wang, F. D'Souza, *J. Phys. Chem. C* **2019**, *123*, 22066–22073.
[47] R. Einholz, T. Fang, R. Berger, P. Grueninger, A. Frueh, T. Chasse, R. F. Fink, H. F. Bettinger, *J. Am. Chem. Soc.* **2017**, *139*, 4435–4442.
[48] E. Kumarasamy, S. N. Sanders, A. B. Pun, S. A. Vaselabadi, J. Z. Low, M. Y. Sfeir, M. L. Steigerwald, G. E. Stein, L. M. Campos, *Macromolecules* **2016**, *49*, 1279–1285.
[49] I. Kaur, W. Jia, R. P. Kopreski, S. Selvarasah, M. R. Dokmeci, C. Pramanik, N. E. McGruer, G. P. Miller, *J. Am. Chem. Soc.* **2008**, *130*, 16274–16286.
[50] T. J. Carey, J. L. Snyder, E. G. Miller, T. Sammakia, N. H. Damrauer, *J. Org. Chem.* **2017**, *82*, 4866–4874.
[51] J. D. Cook, T. J. Carey, N. H. Damrauer, *J. Phys. Chem. A* **2016**, *120*, 4473–4481.

[52] A. D. Thomas, L. L. Miller, *J. Org. Chem.* **1986**, *51*, 4160–4169.
[53] Q. Ye, J. Chang, K.-W. Huang, G. Dai, C. Chi, *Org. Biomol. Chem.* **2013**, *11*, 6285–6291.
[54] I. Kaur, M. Jazdzyk, N. N. Stein, P. Prusevich, G. P. Miller, *J. Am. Chem. Soc.* **2010**, *132*, 1261–1263.
[55] B. Purushothaman, M. Bruzek, S. R. Parkin, A.-F. Miller, J. E. Anthony, *Angew. Chem.* **2011**, *123*, 7151–7155; *Angew. Chem. Int. Ed.* **2011**, *50*, 7013–7017.
[56] G. Mehta, S. Kotha, *Tetrahedron* **2001**, *57*, 625–659.
[57] W. Oppolzer, *Synthesis* **1978**, 793–802.
[58] A. K. Sadana, R. K. Saini, W. E. Billups, *Chem. Rev.* **2003**, *103*, 1539–1602.
[59] I. A. Abdelhamid, H. Butenschön, *Eur. J. Org. Chem.* **2015**, 226–234.
[60] I. A. Abdelhamid, O. M. A. Habib, H. Butenschön, *Eur. J. Org. Chem.* **2011**, 4877–4884.
[61] P. H. Chen, N. A. Savage, G. Dong, *Tetrahedron* **2014**, *70*, 4135–4146.
[62] S. Tripathy, R. Reddy, T. Durst, *Can. J. Chem.* **2003**, *81*, 997–1002.
[63] E. Picazo, K. N. Houk, N. K. Garg, *Tetrahedron Lett.* **2015**, *56*, 3511–3514.
[64] G. Alemayehu, B. Abegaz, W. Kraus, *Phytochemistry* **1998**, *48*, 699–702.
[65] A. L. Zhang, J. C. Qin, M. S. Bai, J. M. Gao, Y. M. Zhang, S. X. Yang, H. Laatsch, *Chin. Chem. Lett.* **2009**, *20*, 1324–1326.
[66] H. Anke, I. Kolthoum, H. Zaehner, H. Laatsch, *Arch. Microbiol.* **1980**, *126*, 223–230.
[67] H. Anke, I. Kolthoum, H. Laatsch, *Arch. Microbiol.* **1980**, *126*, 231–236.
[68] D. H. Hua, K. Lou, S. K. Battina, H. Zhao, E. M. Perchellet, Y. Wang, J.-P. H. Perchellet, *Anti-Cancer Agents Med. Chem.* **2006**, *6*, 303–318.
[69] L. Gross, F. Mohn, N. Moll, P. Liljeroth, G. Meyer, *Science* **2009**, *325*, 1110–1114.
[70] R. Ruiz, D. Choudhary, B. Nickel, T. Toccoli, K.-C. Chang, A. C. Mayer, P. Clancy, J. M. Blakely, R. L. Headrick, S. Iannotta, G. G. Malliaras, *Chem. Mater.* **2004**, *16*, 4497–4508.
[71] R. D. Fedorovich, V. B. Nechytaylo, L. V. Viduta, T. A. Gavrilko, A. A. Marchenko, A. G. Naumovets, A. I. Senenko, P. V. Shabatyn, J. Baran, *Spectrosc. Lett.* **2012**, *45*, 372–377.
[72] C. Santato, R. Capelli, M. A. Loi, M. Murgia, F. Cicoira, V. A. L. Roy, P. Stallinga, R. Zamboni, C. Rost, S. F. Karg, M. Muccini, *Synth. Met.* **2004**, *146*, 329–334.
[73] T. Takahashi, T. Takenobu, J. Takeya, Y. Iwasa, *Adv. Funct. Mater.* **2007**, *17*, 1623–1628.
[74] F. Arcamone, *Med. Res. Rev.* **1984**, *4*, 153–188.
[75] A. A. Moiseeva, *INEOS Open* **2019**, *2*, 9–18.
[76] J. W. Lown, *Chem. Soc. Rev.* **1993**, *22*, 165–176.
[77] R. B. Weiss, G. Sarosy, K. Clagett-Carr, M. Russo, B. Leyland-Jones, *Cancer Chemotherapy Pharmacology* **1986**, *18*, 185–197.
[78] M. Müller, S. Maier, O. Tverskoy, F. Rominger, J. Freudenberg, U. H. F. Bunz, *Angew. Chem.* **2020**, *132*, 1982–1985; *Angew. Chem. Int. Ed.* **2020**, *59*, 1966–1969.
[79] T. Medinger, F. Wilkinson, *Trans. Faraday Soc.* **1965**, *61*, 620–630.
[80] I. Barradas, J. A. Ferreira, M. F. Thomaz, *J. Chem. Soc. Faraday Trans. 2* **1973**, *69*, 388–394.
[81] C. M. Marian, *Annu. Rev. Phys. Chem.* **2021**, *72*, 617–640.
[82] E. G. Azenha, A. C. Serra, M. Pineiro, M. M. Pereira, J. S. De Melo, L. G. Arnaut, S. J. Formosinho, A. M. d. A. R. Gonsalves, *Chem. Phys.* **2002**, *280*, 177–190.
[83] Q. Zhang, H. Kuwabara, W. J. Potscavage, S. Huang, Y. Hatae, T. Shibata, C. Adachi, *J. Am. Chem. Soc.* **2014**, *136*, 18070–18081.
[84] B. Huang, W.-C. Chen, Z. Li, J. Zhang, W. Zhao, Y. Feng, B. Z. Tang, C.-S. Lee, *Angew. Chem.* **2018**, *130*, 12653–12657; *Angew. Chem. Int. Ed.* **2018**, *57*, 12473–12477.
[85] Z. Kuang, G. He, H. Song, X. Wang, Z. Hu, H. Sun, Y. Wan, Q. Guo, A. Xia, *J. Phys. Chem. C* **2018**, *122*, 3727–3737.
[86] J. Choi, D.-S. Ahn, K. Y. Oang, D. W. Cho, H. Ihee, *J. Phys. Chem. C* **2017**, *121*, 24317–24323.
[87] T. Itoh, M. Yamaji, H. Shizuka, *Chem. Lett.* **2000**, 616–617.
[88] T. Itoh, M. Yamaji, H. Shizuka, *Chem. Phys. Lett.* **1997**, *273*, 397–401.
[89] V. Sasirekha, P. Vanelle, T. Terme, C. Meenakshi, M. Umadevi, V. Ramakrishnan, *J. Fluoresc.* **2007**, *17*, 528–539.
[90] E. Apostolova, S. Krumova, T. Markova, T. Filipova, M. T. Molina, I. Petkanchin, S. G. Taneva, *J. Photochem. Photobiol. B* **2005**, *78*, 115–123.
[91] J. Zhang, Z. Chen, L. Yang, F.-F. Pan, G.-A. Yu, J. Yin, S. H. Liu, *Sci. Rep.* **2016**, *6*, 36310pp.
[92] A. Rana, S. Lee, D. Kim, P. K. Panda, *Chem. Eur. J.* **2015**, *21*, 12129–12135.
[93] A. V. Moro, P. C. Ferreira, P. Migowski, F. S. Rodembusch, J. Dupont, D. S. Lüdtke, *Tetrahedron* **2013**, *69*, 201–206.
[94] W. Sun, C. Zhou, C.-H. Xu, Y.-Q. Zhang, Z.-X. Li, C.-J. Fang, L.-D. Sun, C.-H. Yan, *J. Phys. Chem. A* **2009**, *113*, 8635–8646.
[95] B. A. Da Silveira Neto, A. Sant'Ana Lopes, G. Ebeling, R. S. Goncalves, V. E. U. Costa, F. H. Quina, J. Dupont, *Tetrahedron* **2005**, *61*, 10975–10982.
[96] F. Coppola, P. Cimino, U. Raucci, M. G. Chiariello, A. Petrone, N. Rega, *Chem. Sci.* **2021**, *12*, 8058–8072.
[97] F. Siddique, M. Barbatti, Z. Cui, H. Lischka, A. J. A. Aquino, *J. Phys. Chem. A* **2020**, *124*, 3347–3357.
[98] Z.-h. Cui, A. J. A. Aquino, A. C. H. Sue, H. Lischka, *Phys. Chem. Chem. Phys.* **2018**, *20*, 26957–26967.
[99] C. M. Cardona, W. Li, A. E. Kaifer, D. Stockdale, G. C. Bazan, *Adv. Mater.* **2011**, *23*, 2367–2371.
[100] G. W. T. M. J. Frisch, H. B. Schlegel, G. E. Scuseria, M. A. Robb, J. R. Cheeseman, G. Scalmani, V. Barone, G. A. Petersson, H. Nakatsuji, X. Li, M. Caricato, A. V. Marenich, J. Bloino, B. G. Janesko, R. Gomperts, B. Mennucci, H. P. Hratchian, J. V. Ortiz, A. F. Izmaylov, J. L. Sonnenberg, D. Williams-Young, F. Ding, F. Lipparini, F. Egidi, J. Goings, B. Peng, A. Petrone, T. Henderson, D. Ranasinghe, V. G. Zakrzewski, J. Gao, N. Rega, G. Zheng, W. Liang, M. Hada, M. Ehara, K. Toyota, R. Fukuda, J. Hasegawa, M. Ishida, T. Nakajima, Y. Honda, O. Kitao, H. Nakai, T. Vreven, K. Throssell, J. A. Montgomery, Jr., J. E. Peralta, F. Ogliaro, M. J. Bearpark, J. J. Heyd, E. N. Brothers, K. N. Kudin, V. N. Staroverov, T. A. Keith, R. Kobayashi, J. Normand, K. Raghavachari, A. P. Rendell, J. C. Burant, S. S. Iyengar, J. Tomasi, M. Cossi, J. M. Millam, M. Klene, C. Adamo, R. Cammi, J. W. Ochterski, R. L. Martin, K. Morokuma, O. Farkas, J. B. Foresman, D. J. Fox„ Gausian, Inc., Wallingford, CT, **2016**.
[101] J. C. S. Costa, R. J. S. Taveira, C. F. R. A. C. Lima, A. Mendes, L. M. N. B. F. Santos, *Opt. Mater.* **2016**, *58*, 51–60.
[102] W. C. Still, M. Kahn, A. Mitra, *J. Org. Chem.* **1978**, *43*, 2923–2925.

Manuscript received: July 16, 2021
Revised manuscript received: September 3, 2021
Accepted manuscript online: September 3, 2021